THE JOURNAL OF FINANCE • VOL. LVIII, NO. 1 • FEB. 2003

A Monte Carlo Method for Optimal Portfolios

JÉRÔME B. DETEMPLE, RENÉ GARCIA, and MARCEL RINDISBACHER*

ABSTRACT

This paper proposes a new simulation-based approach for optimal portfolio allocation in realistic environments with complex dynamics for the state variables and large numbers of factors and assets. A first illustration involves a choice between equity and cash with nonlinear interest rate and market price of risk dynamics. Intertemporal hedging demands significantly increase the demand for stocks and exhibit low volatility. We then analyze settings where stock returns are also predicted by dividend yields and where investors have wealth-dependent relative risk aversion. Large-scale problems with many assets, including the Nasdaq, SP500, bonds, and cash, are also examined.

The question of optimal portfolio allocation has been of long-standing interest for academics and practitioners in finance. While the mean-variance analysis of Markowitz (1952) is still commonly used among portfolio managers, it has been well understood, since Merton (1971), that long-term investors would prefer portfolios that include hedging components to protect against fluctuations in their investment opportunities. Prompted by the seminal papers of Merton (1969, 1971) and Samuelson (1969), studies have explored various aspects of the dynamic portfolio problem when asset prices follow diffusion processes (e.g., Richard (1975)). This literature has relied, for the most part, on a dynamic programming approach to the problem. More recent contributions by Pliska (1986), Karatzas, Lehoczky, and Shreve (1987), and Cox and Huang (1989) have proposed an alternative resolution method based on martingale techniques. In the context of this approach, an optimal portfolio formula was derived by Ocone and Karatzas (1991). This expression involves expectations of random variables depending on

*Jérôme B. Detemple is at Boston University, School of Management and CIRANO; René Garcia is at Université de Montréal, Department of Economics and CIRANO; and Marcel Rindisbacher is at University of Toronto, Rotman School of Management and CIRANO. The paper was presented at Boston University, Boston College, CIRANO, McMaster University, MIT, NYU (Stern), NYU (Courant), University of Rochester, University of Waterloo, PUC (Rio de Janeiro), York University, The Fields Institute, MITACS general meeting (Toronto), Optimization Days 1999 (Montréal), EFA 1999 (Helsinki), NFA 1999 (Calgary), AFA 2000 (Boston), CMS 2000 (Vancouver), and the 2001 Financial Mathematics conference at UCLA (IPAM). We thank an anonymous referee and the editor, Rick Green, for very useful comments. The paper has also benefited from the suggestions of Helyette Geman, Jacob Sagi, Jun Liu, Larry Epstein, Steve Figlewski, Alex Shapiro, Anthony Lynch, Stan Pliska, Toby Daglish, Martin Gonzales Eiras, David Menagarishvili, and Mark Loewenstein. Financial support from the Network of Centers of Excellence (MITACS) is gratefully acknowledged.

the interest rate (IR) and the market price of risk (MPR) and on unspecified derivatives of these state variables.

While theoretical formulas are available in general contexts, little is known about portfolio properties and, in particular, about the behavior of the hedging terms. Even in the context of diffusion models, realistic specifications with stochastic IR and MPR give rise to complex hedging terms that do not have explicit forms and are difficult to evaluate numerically. As a result, the recent literature on dynamic asset allocation has devoted attention to state variable specifications for which closed-form solutions are available (Kim and Omberg (1996), Liu (2001), Lioui and Poncet (2001), Wachter (2002)), or specifications that are computationally tractable based on dynamic programming techniques (Brennan, Schwartz, and Lagnado (1997), Brennan (1998), Chacko and Viceira (1999), Brennan and Xia (2001), Campbell, Rodriguez, and Viceira (2001)), or discrete time models based on approximated Euler equations (Balduzzi and Lynch (1999), Campbell and Viceira (1999, 2001), Dammon, Spatt, and Zhang (2001)).[1] However, even numerical schemes based on PDEs, which offer the most flexibility, become increasingly difficult to implement when the number of state variables increases. Approximations of the Euler equations, based on a discretization of the state space, suffer from the same curse of dimensionality.

The method proposed here is based on a refinement of the Ocone and Karatzas (1991) formula. It relies on the derivation of explicit expressions for the hedging terms, involving expectations of random variables that can be simulated. The computation of portfolio shares can then proceed using any simulation-based approach. This method is flexible and handles realistic portfolio problems in complete market settings with complex dynamics for the state variables. It permits large numbers of state variables and assets and accommodates wealth-dependent relative risk aversions.

The paper provides three main contributions. First, we exploit the diffusion nature of the state variables processes to derive explicit expressions for the hedging components of the optimal portfolio. Hedging demands are expressed as conditional expectations of random variables that depend on the derivatives of the drift and variance of the relevant state variables. These formulas hold for any structure of the underlying processes and the utility function and reduce the computation of hedging demands to the computation of expectations, as in traditional option pricing theory. Furthermore, they enable us to establish new theoretical results about the hedging behavior. Our approach, which computes the exact solution of the portfolio problem, must be distinguished from recent simulation-based attempts that compute approximations of the optimal portfolio. For instance, Cvitanic, Goukasian, and Zapatero (2003) derive an approximation using the covariation between optimal wealth and the uncertainty shocks and compute the approximate portfolio by simulation. Section 7 documents the convergence and efficiency properties of this method and shows that it is dominated. Brandt, Goyal, and Santa-Clara (2001) also propose a simulation approach to compute an approximation of the optimal portfolio, but in a discrete time

[1] Kogan and Uppal (2000) approximate continuous time solutions.

setting. They combine series expansions of the value function with regressions on powers of the state variables.

Second, we propose a simple transformation of the underlying state variables, which eliminates the stochastic volatility coefficients in the state variable processes. This removes a source of discretization error in simulations of the state variables and improves the rate of convergence. The scheme also increases the speed of convergence of simulated trajectories of hedging terms and of any statistic (such as confidence intervals) of simulated hedging terms.

Third, we provide new results on the economic properties of optimal portfolios. For tractability reasons, recent applied studies of dynamic asset allocation have assumed affine models for the state variables[2] and constant relative risk aversion. In practice, it is well known that the interest rate and the market prices of risk, which are at the core of portfolio choice models, exhibit nonlinearities in their drift and diffusion functions. An IR specification with a nonlinear drift is, for instance, supported by the nonparametric analysis of Aït-Sahalia (1996) and the estimations performed by Ahn and Gao (1999). Similarly, nonlinear patterns in the variance of the market price of risk, such as asymmetric responses to upward and downward price movements or sudden changes in level, are present in the data. Constant relative risk aversion produces demand functions that are proportional to wealth (see Merton (1971)), which does not appear to capture investors' behavior. Researchers have long argued that increasing relative risk aversion seems more plausible (see Arrow (1975)) and that the preservation of a minimum standard of living is a fundamental concern of individuals. Moreover, most personal financial planning advice is wealth dependent. To accommodate these more realistic settings, we examine multivariate nonlinear models of the IR and MPR in settings with constant relative (CRRA) or hyperbolic absolute (HARA) risk aversion.

In our benchmark bivariate model, the IR process has nonlinear mean reversion and constant elasticity of variance (CEV). To model the MPR, we introduce a new class of processes with hyperbolic elasticity of variance, which constitutes a natural generalization of the CEV class. Our MPR process exhibits nonlinear mean reversion and hyperbolic elasticity of variance; a version of this model also allows for an interest rate effect on the drift of the MPR. More elaborate multivariate models with stochastic dividend yield (to capture its predictive power on stock returns) and multiple assets are also examined. In these contexts, we document the magnitude and behavior of the hedging terms as well as their sensitivity to exogenous parameters such as risk aversion, investment horizon, and initial values of the IR and the MPR. All our results are based on a representation of the optimal portfolio evolving from the Ocone–Karatzas formula. This modified formula emphasizes the role of risk aversion and wealth in the hedging terms and sheds further light on the portfolio behavior.

A number of lessons can be drawn from our simulations. Hedging demands are important for asset allocation and tend to increase the demand for stocks. For

[2] The nonparametric approaches of Brandt (1999) and Aït-Sahalia and Brandt (2001) are notable exceptions.

long horizons, intertemporal hedging can easily account for over 60 percent of the stock demand. The IR hedge, which is positive due to negative correlation between the IR and stock returns, overwhelms the MPR hedge, which tends to be negative. This is shown for CRRA in our benchmark model calibrated to the data. The importance of hedging is also documented for HARA utility functions ($u(X) = (1/(1-R))(X+B)^{1-R}$). When marginal utility is finite at zero ($B>0$), the portfolio displays striking differences when the nonnegativity constraint on consumption is enforced. We also find that hedging terms change signs at sufficiently low levels of wealth. These results complement Cox and Huang (1989), who outlined the importance of the constraint for consumption behavior. When the investor is intolerant of wealth shortfalls ($B<0$ and $u(X) = -\infty$ for $X<-B$), hedging becomes even more relevant for the optimal allocation. In the limit, as wealth approaches the present value of the floor, $-B$, the portfolio is entirely motivated by hedging considerations, even for logarithmic utility.

Hedging components exhibit low volatility relative to mean-variance (MV) demands. The IR hedge has the lowest volatility, followed by the MPR hedge and the MV demands. Unlike some earlier studies (e.g., Brennan et al. (1997)), reasonable interior solutions are obtained and portfolio shares are stable in market timing experiments. When the dividend yield is added as a predictor to the IR and the MPR in the drift of the MPR process, its effect on stock demand is marginal. This can be contrasted with Barberis (2000), who finds strong effects of the dividend yield on asset allocation when the benchmark model has i.i.d. returns.

Nonlinearities in the IR-MPR process are not only present in the data, but they also modify the optimal portfolio in a significant manner. Allocation rules based on a mean-reverting square-root IR process and a mean-reverting Gaussian MPR process, calibrated to the data, are biased (biases in excess of 100 percent are recorded in some cases). The size of this bias increases with the investment horizon and the deviation from unit risk aversion. Since nonlinearities reduce the fraction of wealth in the stock, they have a taming effect on the optimal portfolio. This is similar to the effect of parameter uncertainty documented in Barberis (2000).

We also compute and study the optimal portfolio in settings with large numbers of state variables and assets. Simulations of a model with 11 assets and 20 state variables with nonlinear dynamics confirm earlier results: Mutual funds that provide good hedges against IR risk will give rise to particularly large hedging demands. Guidelines for investing in the "New Economy" are also provided. When four asset classes, given by the Nasdaq, S&P500, long-term bonds, and cash, are selected, we find it optimal to short long-term bonds, invest in the S&P500 and Nasdaq, and maintain a positive cash balance. Moreover, we find that holding more stocks for the long run may not be optimal! As the horizon increases, it may become advantageous to reduce the total allocation to the S&P500 and the Nasdaq.

A detailed numerical analysis shows the convergence and efficiency properties of our Monte Carlo estimator, based on Malliavin derivatives in comparison with

PDE methods (as in Brennan et al. (1997)) and other Monte Carlo estimators (Cvitanic et al. (2003)). An experiment shows that our method fares best in terms of root mean square relative errors and maximum absolute errors.

The next section states the portfolio problem. Section II provides the optimal portfolio formula and discusses its structure. Section III presents the change of variables and discusses implementation issues. Section IV introduces a benchmark model and examines the portfolio properties with CRRA. The HARA case and multiasset models are studied in Sections V and VI, respectively. Numerical methods are compared in Section VII. Proofs are in Appendix A; Appendix B reports asymptotic laws of estimators; Appendix C describes the calibration of the models; Appendix D contains a nontechnical introduction to Malliavin calculus for finance.

I. The Portfolio Choice Problem

We consider a portfolio choice problem in a complete market with d state variables Y_{jt}, $j = 1, \ldots, d$, and d sources of Brownian uncertainty W_{it}, $i = 1, \ldots, d$. State variables follow the vector diffusion process[3]

$$dY_t = \mu^Y(t, Y_t)dt + \sigma^Y(t, Y_t)dW_t. \tag{1}$$

The investor allocates his wealth between d risky securities and one riskless asset (a money market account) with instantaneous riskless rate of return $r_t = r(t, Y_t)$. The security prices S_i, $i = 1, \ldots, d$, satisfy the stochastic differential equations

$$dS_{it} = S_{it}[(\mu_i(t, Y_t) - \delta_i(t, Y_t))dt + \sigma_i(t, Y_t)dW_t]; \quad 1 \leq i \leq d, \tag{2}$$

where μ_i is the expected return, δ_i the dividend rate, and σ_i the vector of volatility coefficients of security i. Let σ denote the $d \times d$-dimensional volatility matrix whose rows are σ_i, $i = 1, \ldots, d$. We assume that σ is invertible and that the market price of risk

$$\theta_t = \theta(t, Y_t) \equiv \sigma(t, Y_t)^{-1}(\mu(t, Y_t) - r(t, Y_t)\mathbf{1}), \tag{3}$$

where $\mathbf{1}$ is the unit vector, is continuously differentiable, and satisfies the Novikov condition $E\exp\left(\frac{1}{2}\int_0^T \theta_t'\theta_t\, dt\right) < \infty$. Under this condition, the state price density is

$$\xi_t \equiv \exp\left[-\int_0^t r_s\, ds - \int_0^t \theta_s' dW_s - \frac{1}{2}\int_0^t \theta_s'\theta_s\, ds\right]. \tag{4}$$

Relative state prices are written $\xi_{t,v} \equiv \xi_v/\xi_t = \exp(-\int_t^v (r_s + \frac{1}{2}\theta_s'\theta_s)ds - \int_t^v \theta_s dW_s)$.

Suppose that an investor seeks to maximize the expected utility of terminal wealth by selecting a dynamic portfolio policy composed of the d risky assets

[3] We assume that the coefficients of (1) satisfy Growth and Lipschitz conditions. Note also that the state variables are joint solutions of the system (1), that is, state variables can influence each other.

and the riskless asset

$$\max_{\pi} U(X_T) \equiv E[u(X_T)] \quad s.t. \tag{5}$$

$$\begin{cases} dX_t = r_t X_t dt + X_t \pi_t'[(\mu_t - r_t \mathbf{1})dt + \sigma_t dW_t], \quad X_0 = x \\ X_t \geq 0 \text{ for all } t \in [0, T]. \end{cases} \tag{6}$$

Here X_t represents the investor's wealth at date t, x is initial wealth, and π_t the proportions invested in the risky assets at date t. The nonnegativity constraint is a typical no-bankruptcy condition. The utility function is strictly increasing and concave with limits $\lim_{x \to \infty} u'(x) = 0$ and $\lim_{x \to 0} u'(x) \leq \infty$. Since we allow for finite marginal utility of consumption at zero, utility specifications such as those with hyperbolic absolute risk aversion are permitted.

II. The Optimal Portfolio: The Hedging Behavior

This portfolio problem has been resolved by using a martingale approach that identifies optimal terminal wealth explicitly (Karatzas et al. (1987), Cox and Huang (1989)). An application of the Clark–Ocone formula then gives the financing portfolio. This approach, adopted by Ocone and Karatzas (1991), expresses the portfolio in the form of conditional expectations of random variables. Given the generality of their model in which the drift and the volatility of returns are not modeled explicitly, these random variables are left unspecified. In this section, we show that the diffusion nature of the financial market can be used to derive explicit expressions for these random terms, and hence for the portfolio shares.

A. The Optimal Portfolio Policy

Our first result identifies the general structure of the optimal portfolio and of its hedging components. Let $R(x) \equiv -u''(x)x/u'(x)$ be the (atemporal) Arrow–Pratt measure of relative risk aversion. With this notation, we have the following theorem.

THEOREM 1: *The optimal portfolio shares are given by*

$$\pi_t = (\sigma(t, Y_t)')^{-1} \left[\frac{1}{R(X_t)} \theta(t, Y_t) c(t, X_t, Y_t) - a(t, X_t, Y_t) - b(t, X_t, Y_t) \right] \tag{7}$$

where

$$a(t, X_t, Y_t)' \equiv \mathbf{E}_t \left[\xi_{t,T} \frac{X_T}{X_t} \left(1 - R(X_T)^{-1} \right) 1_{X_T > 0} \int_t^T \mathcal{D}_t r_s \, ds \right] \tag{8}$$

$$b(t, X_t, Y_t)' \equiv \mathbf{E}_t \left[\xi_{t,T} \frac{X_T}{X_t} \left(1 - R(X_T)^{-1} \right) 1_{X_T > 0} \int_t^T (dW_s + \theta_s \, ds)' \mathcal{D}_t \theta_s \right] \tag{9}$$

$$c(t,\, X_t,\, Y_t) \equiv \mathbf{E}_t\left[\xi_{t,\,T}\frac{X_T}{X_t}\frac{R(X_t)}{R(X_T)}1_{X_T>0}\right]. \tag{10}$$

In these expressions optimal wealth equals $X_t = \mathbf{E}_t[\xi_{t,\,T}I(y\xi_T)^+]$*, where* $I(\cdot)$ *is the inverse marginal utility function,* $I(\cdot)^+ = \max\{I(\cdot), 0\}$*, and* y *solves* $x = \mathbf{E}[\xi_T I(y\xi_T)^+]$*. The symbol* $1_{X_T>0}$ *is the indicator of the event* $\{X_T > 0\}$*. The random variables* $\mathcal{D}_t r_s$ *and* $\mathcal{D}_t\theta_s$ *in (8) and (9) are Malliavin derivatives.*[4] They are given by $\mathcal{D}_t\theta_s' = \partial_2\theta(s,\, Y_s)'\mathcal{D}_t Y_s$ *and* $\mathcal{D}_t r_s = \partial_2 r(s,\, Y_s)\mathcal{D}_t Y_s$*, where* $\mathcal{D}_t Y_s = (\mathcal{D}_{1t}Y_s, \ldots, \mathcal{D}_{dt}Y_s)$ *solves the linear stochastic differential equation*

$$d(\mathcal{D}_{kt}Y_s) = \partial_2\mu^Y(s,\, Y_s)\mathcal{D}_{kt}Y_s ds + \left(\sum_{j=1}^{d}\partial_2\sigma_{\cdot j}^Y(s,\, Y_s)dW_{js}\right)\mathcal{D}_{kt}Y_s, \tag{11}$$

subject to the boundary condition $\lim_{s\to t}\mathcal{D}_{kt}Y_s = \sigma_{\cdot k}^Y(t,\, Y_t)$*. In (11),* $\sigma_{\cdot j}^Y$ *is the* j^{th} *column of the matrix* σ^Y *and* $\partial_2\sigma_{\cdot j}^Y(s,\, Y_s)$ *is the gradient with respect to* Y_s *of* $\sigma_{\cdot j}^Y(s,\, Y_s)$*,* $j = 1, \ldots d$*.*[5]

The contribution of Theorem 1, relative to Ocone and Karatzas (1991), is to show that the Malliavin derivatives of the state variables satisfy diffusion processes. This result is especially important for the numerical implementation of the formula. Indeed, the diffusion evolution (11) implies that simulation methods can be used to calculate the portfolio shares.

An important ingredient in the portfolio formula is the Malliavin derivatives $(\mathcal{D}_{1t}Y_s, \ldots, \mathcal{D}_{dt}Y_s)$ of the state variables. The random variable $\mathcal{D}_{kt}Y_s$ captures the impact of an innovation in the Brownian motion W_k at time t on the state variable Y_s at time s. In essence, this derivative measures the persistence of a shock in the state variable. It is similar to an impulse response function that quantifies the sensitivity of a variable Y_s to a past uncertainty shock at time t.

The first component of the portfolio (7) is a mean-variance term, while the next two are intertemporal hedging terms (see Merton (1971)).[6] In this general setting, the mean-variance demand varies with optimal wealth, since relative risk aversion depends on wealth. Hedging arises as the investor seeks insurance against fluctuations in the IR (second term in (7)) and in the MPR (third term in (7)). The interpretation of the second term follows from the presence of the Malliavin derivative $\mathcal{D}_t r_s$. As indicated above, this derivative captures the effect of shocks at t on the value of the interest rate r_s at the future date s. It measures the IR's

[4] The Malliavin derivative is a generalized notion of derivative that extends the usual concept to path-dependent functions. Just as the ordinary derivative measures the local change of a function for a small change in the underlying variable, the Malliavin derivative measures the change in a path-dependent function implied by a small change in the path of the underlying Brownian motion. See Appendix D for a short introduction to Malliavin calculus.

[5] We assume that the value function associated with (5) – (6) is finite, $V(x) < \infty$, and that $\xi_T I(y\xi_T) \in \mathbb{D}^{1,2}$, where $\mathbb{D}^{1,2}$ is the domain of the Malliavin derivative (see Nualart (1995) for complete definitions).

[6] The optimal portfolio formula extends to the case of intermediate consumption. It also extends to infinite horizon provided that the Novikov condition is satisfied.

sensitivity to the underlying risk factors, that is, the Brownian motions W_i. Similarly, the third term containing $\mathcal{D}_t\theta_s$ is an MPR hedge. It is present whenever the MPRs are sensitive to W_i. When (r, θ) are constant or deterministic, these derivatives are null and the hedging terms disappear. When the opportunity set is stochastic, (r, θ) depend on Y and become sensitive to past innovations in the state variables. The Malliavin derivatives $\mathcal{D}_t r_s, \mathcal{D}_t\theta_s$ then differ from zero and hedging matters for the optimal allocation.

When relative risk aversion is constant, the optimal portfolio is given by (7), where $c(t, X_t, Y_t) = 1$ and where the functions $a(\cdot)$ and $b(\cdot)$ are independent of wealth and equal to

$$a(t,\ Y_t)' \equiv \rho \mathbf{E}_t\left[\frac{\xi^{\rho}_{t,T}}{\mathbf{E}_t[\xi^{\rho}_{t,T}]}\int_t^T \mathcal{D}_t r_s\, ds\right] \tag{12}$$

$$b(t,\ Y_t)' \equiv \rho \mathbf{E}_t\left[\frac{\xi^{\rho}_{t,T}}{\mathbf{E}_t\left[\xi^{\rho}_{t,T}\right]}\int_t^T (dW_s + \theta_s\, ds)'\mathcal{D}_t\theta_s\right], \tag{13}$$

with $\rho \equiv 1 - 1/R$ constant. These expressions are obtained by using the relation between optimal wealth and state prices to write a, b in terms of the relative state price density $\xi_{t,T}$. These formulas, which are a restatement of (4.21) in Ocone and Karatzas (1991), show that, with CRRA, the functions a, b are independent of wealth. They will be used in some of our numerical computations.

B. The Intertemporal Hedging Behavior

Let us now focus on the hedging behavior of the investor. First, note that an individual with logarithmic utility ($R(X_t) = 1$) does not hedge. The signs of the hedging terms will otherwise depend on the signs of the conditional expectations $a(t, X_t, Y_t)$ and $b(t, X_t, Y_t)$. For the IR hedge, simple sufficient conditions ensure an unambiguous behavior.

PROPOSITION 1: Fix $t \in [0, T]$. *Suppose that (i)* $(\sigma(t,\ Y_t)')^{-1}(\mathcal{D}_t r_s)' \leq 0$ *for all* $s \geq t$, *(P-a.s) and that (ii)* $R(X_T) \geq 1$ *(P-a.s). Then, intertemporal hedging of interest rate risk raises the demand for stocks (i.e., the IR hedge is nonnegative). If (i) and (ii) hold for all* $t \in [0, T]$, *the IR hedge boosts the proportion of wealth invested in stocks at all times.*

These two conditions support the intuitive notion that individuals that are more risk averse than a log investor ($R(X_T) \geq 1$) will increase their demand for the market portfolio when the IR covaries negatively with the market return (single risky asset model) in order to hedge IR risk. The first condition holds in a variety of special cases that are of interest for empirical or theoretical reasons. For instance, it holds if the dynamics of the state variables are independent of each other (i.e. $\mu^{Yj}(t, Y_{jt})$ and $\sigma^{Yj}(t, Y_{jt})$ do not depend on Y_i, $i \neq j$) and

$$(\sigma(t,\ Y_t)')^{-1}\left(\partial_2 r(t,\ Y_t)\sigma^Y(t,\ Y_t)\right)' \leq 0. \tag{14}$$

In the single risky asset case, this boils down to *negative correlation* between the IR and the risky asset price, which is empirically verified if the risky asset is interpreted as the S&P500 index. The second condition is stated for models in which relative risk aversion varies with optimal wealth. As long as an investor displays more risk aversion than a myopic investor, for all possible realizations of optimal terminal wealth, the condition will hold.

In the next section, we explain how to obtain quantitative estimates of the optimal portfolio shares and of the hedging terms using a Monte Carlo procedure based on Malliavin derivatives.

III. Computation of Portfolios and Hedging Terms

We first outline the numerical procedure employed to implement the portfolio formula. We then present an alternative procedure based on a change of variables and document the benefits of this modified approach in a numerical experiment.

A. A Monte Carlo Portfolio Estimator

To implement the portfolio formula (7), we need to compute the functions $a(\cdot)$, $b(\cdot)$, and $c(\cdot)$, which are conditional expectations of random variables depending on the paths of the state variables Y_s and their Malliavin derivatives $\mathcal{D}_t Y_s$. An expansion of the state space enables us to treat these random variables as diffusion processes that can be simulated along with $(Y_s, \mathcal{D}_t Y_s)$.

For illustration purposes, we focus on the formulas (12) and (13) for CRRA. The random variables in the hedging terms form a joint system $(Y_s, \mathcal{D}_t Y_s, \xi_{t,s}, H^r_{t,s}, H^\theta_{t,s})$, where $H^r_{t,s} \equiv \int_t^s \mathcal{D}_t r_v dv$ and $H^\theta_{t,s} \equiv \int_t^s (dW_v + \theta_v dv)' \mathcal{D}_t \theta_v$. A standard application of Ito's lemma gives

$$d\xi_{t,s} = -\xi_{t,s}\big(r(s, Y_s)ds + \theta(s, Y_s)' dW_s\big) \tag{15}$$

$$dH^r_{t,s} = \partial_2 r(s, Y_s) \mathcal{D}_t Y_s ds \tag{16}$$

$$dH^\theta_{t,s} = (dW_s + \theta(s, Y_s)ds)' \partial_2 \theta(s, Y_s) \mathcal{D}_t Y_s, \tag{17}$$

where $(Y_s, \mathcal{D}_t Y_s)$ solve (1) and (11).

For implementation purposes, M trajectories of the solutions of these equations are simulated simultaneously. This can be performed using a standard Euler scheme that discretizes the time interval in N points. The result is a set of M estimates $(Y_s^{N,i}, \mathcal{D}_t^{N,i} Y_s, \xi_{t,s}^{N,i}, H_{t,s}^{r,N,i}, H_{t,s}^{\theta,N,i})$, one per trajectory, of the random variables in the hedges, which can be used to construct M estimates, $(\xi_{t,s}^{N,i})^\rho H_{t,s}^{r,N,i}$ and $(\xi_{t,s}^{N,i})^\rho H_{t,s}^{\theta,N,i}$, of $\xi^\rho_{t,s} H^r_{t,s}$ and $\xi^\rho_{t,s} H^\theta_{t,s}$. Averaging over these M quantities provides estimates of the functions $a(\cdot)$ and $b(\cdot)$ in the hedges

$$\hat{a}(t, Y_t)' = \frac{\sum_{i=1}^M (\xi_{t,T}^{N,i})^\rho H_{t,T}^{r,N,i}}{\sum_{i=1}^M (\xi_{t,T}^{N,i})^\rho} \quad \text{and} \quad \hat{b}(t, Y_t)' = \frac{\sum_{i=1}^M (\xi_{t,T}^{N,i})^\rho H_{t,T}^{\theta,N,i}}{\sum_{i=1}^M (\xi_{t,T}^{N,i})^\rho}. \tag{18}$$

The precision of these estimators depends on the number of Monte Carlo replications M and the number of time discretization points N. As shown in Detemple, Garcia, and Rindisbacher (DGR) (2001), convergence to the true values is at the rate $1/\sqrt{M}$ as long as the ratio $\sqrt{M}/N$ is held constant. For a single Monte Carlo replication, the Euler scheme converges weakly at rate $1/\sqrt{N}$ for diffusion processes.[7,8]

A drawback of this approach is that the processes to be simulated have stochastic components depending on the state variables. As shown in DGR (2001), the presence of these terms slows down the convergence of numerical estimates to their true value. In turn, this increases the demands placed on the computational procedure in order to achieve a given level of accuracy. In the next section, we propose a simple reformulation of the model, which simplifies (or eliminates) the stochastic terms in the simulated processes and, therefore, improves the convergence speed to the true values.

B. A Variance Stabilizing Transformation for the Hedging Terms

The key to this reformulation is a change of variables that normalizes the volatility of a process to a constant.[9] Suppose that a state variable Y satisfies the one-dimensional version of (1), where W is a single Brownian motion. Following Doss (1977), we introduce a new state variable $Z_t = F(t, Y_t)$, where the function $F : [0, T]\times\mathbb{R}\mapsto\mathbb{R}$ is selected so that $\partial_2 F = 1/\sigma^Y$. Using Ito's lemma shows that Z satisfies (see Appendix A for details)

$$dZ_t = m(t, Z_t)dt + dW_t, \tag{19}$$

where $m(t, Z) \equiv \left[\mu/\sigma - \frac{1}{2}\partial_2\sigma + \partial_1 F\right](t, Y)$ with $Y = F^{-1}(t, Z)$. Since the equation has unit variance, there is no need to approximate the volatility of the process, and this will improve the convergence properties of the simulation scheme. Moreover, taking the Malliavin derivative on each side gives

$$d\mathcal{D}_t Z_s = \partial_2 m(s, Z_s)\mathcal{D}_t Z_s ds, \quad \text{subject to} \quad \mathcal{D}_t Z_t = 1. \tag{20}$$

This linear equation for $\mathcal{D}_t Z_s$ does not have a stochastic part and is therefore easy to simulate. Finally, since there is a one-to-one correspondence between Z and Y, we can express the portfolio formulas entirely in terms of the pair $(Z_s, \mathcal{D}_t Z_s)$.[10] This is accomplished as follows in Proposition 2.

PROPOSITION 2: *Suppose that (i) the drift μ^Y is continuously differentiable in (t, Y), (ii) the volatility σ^Y is twice continuously differentiable in (t, Y), and (iii) $\mu^Y(t, 0)$ and $\sigma^Y(t, 0)$ are bounded for all $t\in[0, T]$. Then, for all $t\leq s$, we obtain*

[7] A sequence of random variables Z^N *converges weakly to* Z *at the rate* $1/\sqrt{N}$ if $\sqrt{N}(Z^N - Z) \Rightarrow U^Z \neq 0$, where convergence is in probability and U^Z is the error. See Appendix B for asymptotic laws of state variables estimators and DGR (2001) for further details.

[8] See Kurtz and Protter (1991).

[9] Doss (1977) used the transformation to show that an SDE can be solved pathwise.

[10] An extension of these results to multiple state variables is available from the authors.

$\mathcal{D}_t Y_s = \sigma^Y(s, Y_s)\mathcal{D}_t Z_s$ *with*

$$\mathcal{D}_t Z_s = \exp\left[\int_t^s \partial_2 m(t, Z_v)dv\right]. \tag{21}$$

Proposition 2 shows that $(Y_s, \mathcal{D}_t Y_s)$ can be written in terms of $(Z_s, \mathcal{D}_t Z_s)$. Since (21) depends only on Riemann–Stieltjes integrals, of first and second derivatives of the coefficients of Y, stochastic integrals have been eliminated. With this "variance-stabilizing" transformation, the numerical calculation of the random variable $\mathcal{D}_t Y_s$ is of the same complexity as the numerical solution of an ODE. The result is a faster convergence speed equal to $1/N$, which is due to the absence of a stochastic integral in the ODE.

Implementation can now proceed as in Section III.A. The only modification is that we simulate the pair $(Z_s, \mathcal{D}_t Z_s)$ to get approximate trajectories $(Z_s^{N,i}, \mathcal{D}_t^{N,i} Z_s)$ and use the inverse function $F^{-1}(s, Z_s)$ and Proposition 2 to get estimates $Y_s^{N,i} = F^{-1}(s, Z_s^{N,i})$ of the original state variables and $(\mathcal{D}_t^{N,i} Y_s, \xi_{t,s}^{N,i}, H_{t,s}^{r,N,i}, H_{t,s}^{\theta,N,i})$ of the random variables in the hedges.

C. Simulation Results

We now illustrate the difference in performance between the approaches with and without transformation, for the approximation of Malliavin derivatives. Suppose that we compute the derivative $\mathcal{D}_0 r_T$, using each of the two methods. Absolute computational errors are estimated for different discretizations N of the time interval $[0, T]$ by the strong criterion

$$\hat{\varepsilon}(N, M) = \hat{E}^M\left|\mathcal{D}_0^N r_T - \mathcal{D}_0 r_T\right| = \frac{1}{M}\sum_{i=1}^{M}\left|\mathcal{D}_0^{N,i} r_T - \mathcal{D}_0^i r_T\right|, \tag{22}$$

where $\mathcal{D}_0 r_T$ is the true value of the derivative and $\mathcal{D}_0^N r_T$ its approximation, based on N discretization points using M independent replications. We also compute the respective errors with and without transformation for the state variable r_T. Since the computation of the statistic $\hat{\varepsilon}(N, M)$ requires the true distribution of the Malliavin derivative, we assume that the IR follows a special case of the general mean reverting process with *hyperbolic elasticity of variance* introduced in the next section (see (23) with $\gamma_r = \frac{1}{2}$), with parameters $T = 1$, $\kappa_r = 0.004$, $\bar{r} = 0.06$, $\sigma_r = 0.0309839$, and $r_0 = 0.06$.[11] To calculate the expectation above, we take 20 batches of 1,000 simulations each. For each batch, an absolute error is estimated.

[11] Since $\sigma_r = 2\sqrt{\kappa_r \bar{r}}$, the IR is the square of an Ornstein–Uhlenbeck process $Y_t = \sqrt{r_t}$. The true value can then be calculated by using the exact simulation of the transformed state variables

$$Y_{t+\Delta} = Y_t e^{\alpha\Delta} + \beta(\sigma_r e^{\alpha\Delta}\sqrt{\Delta}(W_{t+\Delta} - W_t) + \sqrt{|s_{22}|}Z),$$

where Z is a Gaussian variate independent of W, $\alpha = -\frac{\kappa_r}{2}$, $\beta = \sigma_r/2, \Delta = T/N$, and $s_{22} = e^{2\alpha\Delta}(1/2\alpha - \Delta) + 2(\Delta - 1/\alpha) + 3/2\alpha$. This choice of coefficients ensures that Y has the correct variance and covariance with the increment of the Brownian motion $W_{t+\Delta} - W_t$.

Table I

Comparison of the Speeds of Convergence of the Discretization Schemes When the IR follows a MRSR Process

This table compares the mean absolute errors of the Euler discretization scheme (Euler) and of the discretization scheme based on the variance stabilizing transformation (Euler-Transform) as the number of discretization points (N) increases. The errors are reported for the level of the interest rate (IR) r and of the Malliavin derivative $\mathcal{D}r$. Errors are computed with respect to the true distributions of r and $\mathcal{D}r$, which are known for the mean reverting square root (MRSR) process chosen. The mean is computed over 20 batches of 1,000 simulations each.

N	r		$\mathcal{D}r$	
	Euler	Euler-Transform	Euler	Euler-Transform
2	0.000115598	5.49255e-06	5.81463e-07	3.47457e-07
4	0.000111128	3.37985e-06	3.58341e-07	2.13681e-07
8	8.74541e-05	1.82631e-06	2.33208e-07	1.15422e-07
16	6.50156e-05	9.41716e-07	1.6312e-07	5.9616e-08
32	4.66084e-05	4.7979e-07	1.16983e-07	3.03396e-08
64	3.336e-05	2.40698e-07	8.29213e-08	1.52396e-08
128	2.3761e-05	1.20386e-07	5.97503e-08	7.63041e-09
256	1.68824e-05	5.83759e-08	4.18739e-08	3.69586e-09
512	1.19618e-05	2.53747e-08	3.00371e-08	1.60477e-09

Estimated absolute errors are then averaged over the batches. Table I reports the results. Columns 2 and 4 show that the speed of convergence of the Euler scheme is roughly of order $1/\sqrt{N}$. Columns 3 and 5 illustrate the increase in convergence speed to $1/N$ when the transformation is used.

This numerical example illustrates the theoretical result (see Appendix B) and confirms the improvement in the speed of convergence when the transformation is applied. The gain is of primary importance in exercises involving the simulation of hedging terms and of optimal portfolios over time, such as market timing experiments.[12]

IV. A Benchmark Model with Nonlinear Coefficients

This section both formulates a new model rich enough to capture salient nonlinear features of the data and examines the properties of optimal portfolios.

A. The Model: Nonlinear Mean Reversion and Elasticity of Variance

The evolution of the investment opportunity set is described by the pair of state variables (r, θ) which satisfy[13]

$$dr_t = \kappa_r(\bar{r} - r_t)\left(1 + \phi_r(\bar{r} - r_t)^{2\eta_r}\right)dt - \sigma_r r_t^{\gamma_r} dW_t, \quad r_0 \text{ given} \tag{23}$$

[12] When the conditioning state variables are known, estimates of conditional expectations based on the two schemes, with and without transformation, converge at the same speed (see DGR (2001)).

[13] This is equivalent to a model with two state variables $Y = (Y_1, Y_2)$ in which the equations $(r_t = r(t, Y_1), \theta_t = \theta\,(t, Y_2))$ can be inverted and the state variables expressed as $Y_t = (f_1(r_t), f_2(\theta_t))$.

$$d\theta_t = \big(\kappa_\theta(\bar{\theta} - \theta_t) + \mu_\theta^r(r_t, \theta_t)\big)dt + \sigma_\theta(\theta_t)dW_t, \quad \theta_0 \text{ given}, \tag{24}$$

where

$$\mu_\theta^r(r_t, \theta_t) \equiv \delta_r(\bar{r} - r_t)(\theta_l + \theta_t)\left(1 - \left(\frac{\theta_l + \theta_t}{\theta_l + \theta_u}\right)\right) \tag{25}$$

$$\sigma_\theta(\theta_t) = \sigma_\theta(\theta_l + \theta_t)^{\gamma_{1\theta}}\left(1 - \left(\frac{\theta_l + \theta_t}{\theta_l + \theta_u}\right)^{1-\gamma_{1\theta}}\right)^{\gamma_{2\theta}}. \tag{26}$$

The coefficients $(\kappa_r, \bar{r}, \phi_r, \eta_r, \sigma_r, \gamma_r, \kappa_\theta, \bar{\theta}, \eta_\theta, \sigma_\theta, \theta_l, \theta_u, \gamma_{1\theta}, \gamma_{2\theta})$ are constants, $(\kappa_r, \bar{r}, \kappa_\theta, \theta_l, \theta_u)$ are positive, and $\bar{\theta} \in (-\theta_l, \theta_u)$. The Brownian motion W is unidimensional.

The IR process (23) is mean reverting with constant elasticity of variance (NMRCEV) given by $-2\gamma_r$. It also exhibits nonlinearities in the speed of mean reversion that are captured by the function $\phi_r(\bar{r} - r_t)^{2\eta_r}$. This specification, with nonlinear drift and volatility, is motivated by the nonparametric analysis of Ait-Sahalia (1996). IR processes of the form (23) but with a linear drift—that is, constant speed of mean reversion ($\phi_r = 0$)—were used in another context in Chan et al. (1992); the Cox, Ingersoll, and Ross (1985) model is a particular member of this class with square-root volatility ($\phi_r = 0$, $\gamma_r = 0.5$). IR models with quadratic drift—that is, linear speed of mean reversion ($\phi_r \neq 0$ and $\eta_r = \frac{1}{2}$)—were introduced by Ahn and Gao (1999). More general models with $\phi_r \neq 0$ and $\eta_r \neq \frac{1}{2}$ have yet to be explored.

The MPR process exhibits mean reversion and has an elasticity of variance given by[14]

$$\varepsilon(x) = -2\frac{x}{\theta_l + x}\left[\gamma_{1\theta} - \gamma_{2\theta}(1 - \gamma_{1\theta})\frac{\left(\frac{\theta_l + x}{\theta_l + \theta_u}\right)^{1-\gamma_{1\theta}}}{1 - \left(\frac{\theta_l + x}{\theta_l + \theta_u}\right)^{1-\gamma_{1\theta}}}\right]. \tag{27}$$

The left panel of Figure 1 shows that the elasticity of variance is hyperbolic in the neighborhood of the points $-\theta_l$ and θ_u. This reflects the convergence of the volatility to zero as θ approaches $-\theta_l$ and θ_u. Typical volatility patterns are illustrated in the right panel. The volatility function is concave with a maximum at $(\gamma_{1\theta}/(\gamma_{1\theta} + \gamma_{2\theta}(1 - \gamma_{1\theta})))^{1/(1-\gamma_{1\theta})}$. The parameters $\gamma_{1\theta}, \gamma_{2\theta}$ control the degree of skewness toward the left or right. The function $\mu_\theta^r(r_t, \theta_t)$ in the drift of the MPR captures an interest rate dependence (empirically a good predictor of the MPR). This formulation ensures that the MPR stays between the two reflecting bounds $-\theta_l$ and θ_u at all times. In view of these properties, the process is said to exhibit mean reversion with hyperbolic elasticity of variance and interest rate dependence in the drift (MRHEVID). CEV processes, introduced by Cox and Ross (1976) for option pricing, are a subcase of our model for the MPR obtained by setting

[14] The elasticity of variance, $\varepsilon \equiv -(\partial v(x)/\partial x)/(v(x)/x)$, measures the relative change in the variance $v(x) = \sigma^2(x)$. The elasticity of variance is said to be *hyperbolic* when $\varepsilon \simeq k(1 + mx)^{-n}$ with k, m and $n > 0$ constants.

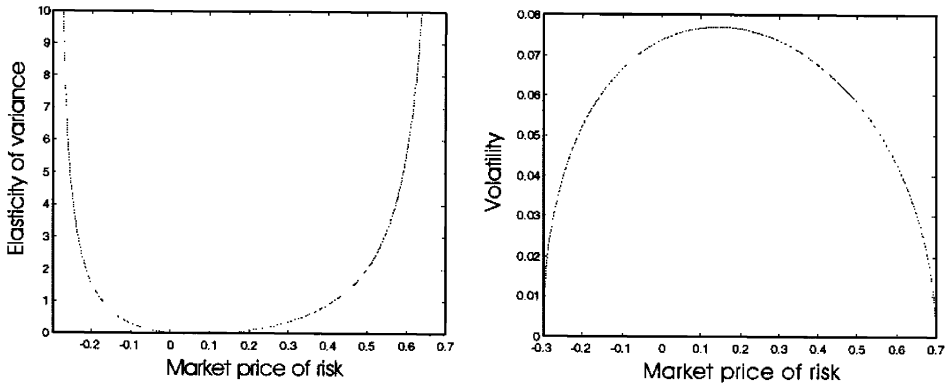

Figure 1. The hyperbolic elasticity of variance (HEV) process. Elasticity of variance (left panel), volatility function (right panel). Parameters: $\theta_l = 0.3$, $\theta_u = 0.7$, $\gamma_{1\theta} = \gamma_{2\theta} = 0.5$.

$\theta_l = \gamma_{2\theta} = 0$. General specifications with hyperbolic absolute elasticity of variance ($\theta_l \neq 0$ and $\gamma_{2\theta} \neq 0$) are new.

The bivariate specification (23) and (24) for the IR and the MPR is new in the literature. While modeling directly the two processes of interest, our structure captures important nonlinearities in the mean and volatility of these variables, which are present in the data. This general specification will enable us to assess the importance of those nonlinearities for portfolio decisions, a question that has not yet been explored.

The transition from the model with state variables Y to the model (23) and (24) with state variables (r, θ) is immediate. Proposition 2 applies, substituting the relevant expressions for the derivatives of the drift and volatility in (21). These derivatives are given in Appendix A.

B. Economic Properties of Optimal Portfolios

We implement our procedure for the benchmark model with CRRA and a single risky stock with constant volatility. Details of the calibration and parameter values are in Appendix C. Initial values are $r_0 = 0.06$ and $\theta_0 = 0.10$, while the volatility of the stock is set at its historical average 0.2. Through most of the paper simulations, we use a three-day increment and 50,000 paths with variance reduction by antithetic variables ($M = 25{,}000$, $h = 1/100$).

B.1. Optimal Portfolios and Hedging Components

Figure 2 (see also Table II) illustrates the behavior of the optimal portfolio and its components relative to the risk aversion and the investment horizon. Risk aversion varies from 0.5 to 5; the horizon from 1 to 10 years. As expected, the fraction of wealth in the stock is a decreasing (increasing) function of risk aversion (the horizon). The hedges, however, display very different behavior. The MPR hedge is mildly humped, decreasing-increasing, relative to risk aversion, while the IR hedge is increasing in that variable. Both hedges increase in absolute

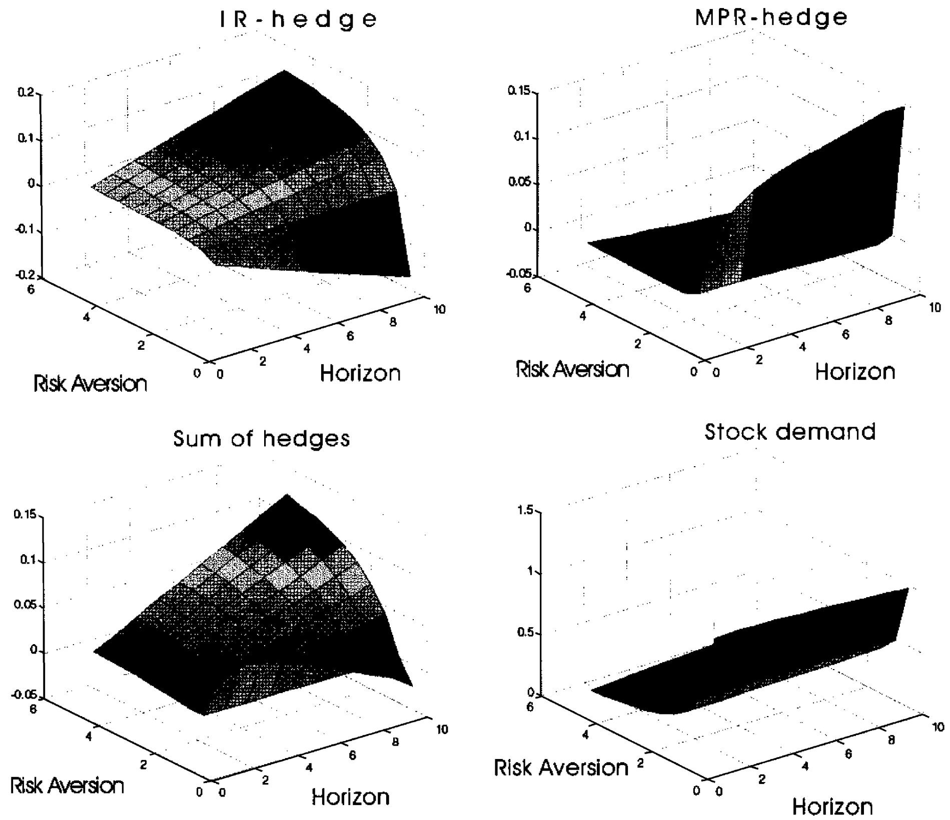

Figure 2. Effects of investment horizon and risk aversion on total stock demand and hedging demands. Interest rate hedging (IRH) demand (top left), market price of risk hedging (MPRH) demand (top right), total hedging demand (bottom left), total demand (bottom right).

value as the horizon increases. As noted before, hedges change signs as risk aversion exceeds or falls short of 1, illustrating the knife-edge behavior of logarithmic utility. For investors that are more risk averse than the Bernoulli investor, the negative values of the MPR hedge stem from the positive correlation between the stock return and the MPR. The additional risk is hedged by reducing the stock demand. Similarly, the IR hedge tends to boost stock demand, since it covaries negatively with the stock return. Note that the combination of the two hedges tends to be positive: hedging increases stock holdings relative to a pure mean-variance investor. In fact, the positive net effect increases with the horizon, when risk aversion exceeds 1. This dominance of the IR hedge reflects the stronger persistence of IR shocks (slower mean reversion).

Figure 3 displays the behavior relative to the levels of the IR and MPR for a risk aversion of 3 and an investment horizon of five years. Note that the fraction invested in the stock is an increasing function of the MPR and is almost insensitive to the IR. As θ_0 increases, the IR hedge stays flat (top left panel), while the MPR

Table II

Shares of the Portfolio in the Stock and Hedging Components

This table reports the optimal share of the portfolio invested in the stock (π), the interest rate hedge (IRH), and the market price of risk hedge (MPRH) for different risk aversions (R) and horizons (T). Computations are performed in the bivariate benchmark model with IR and MPR state variables and two sources of uncertainty. The IR process is mean reverting with constant elasticity of variance and exhibits nonlinearities in the speed of mean reversion. The MPR process exhibits mean reversion with hyperbolic elasticity of variance and interest rate dependence in the drift. The values of the parameters for the processes are given in Appendix C.

R		T					
		1	2	3	4	5	10
0.5	π	1.0398	1.0489	1.0440	1.0354	1.0237	0.9627
	IRH	− 0.0196	− 0.0388	− 0.0577	− 0.0763	− 0.0946	− 0.1819
	MPRH	0.0594	0.0876	0.1017	0.1117	0.1184	0.14469
1	π	0.5000	0.5000	0.5000	0.5000	0.5000	0.5000
	IRH	0.0000	0.0000	0.0000	0.0000	0.0000	0.0000
	MPRH	0.0000	0.0000	0.0000	0.0000	0.0000	0.0000
2	π	0.2529	0.2594	0.2670	0.2754	0.2837	0.3236
	IRH	0.0098	0.0195	0.0292	0.0387	0.0481	0.0939
	MPRH	− 0.0069	− 0.0101	− 0.0121	− 0.0133	− 0.0144	− 0.0202
4	π	0.1343	0.1462	0.1590	0.1715	0.1845	0.2445
	IRH	0.0147	0.0293	0.0438	0.0582	0.0724	0.1413
	MPRH	− 0.0054	− 0.0081	− 0.0099	− 0.0117	− 0.0129	− 0.0218

hedge is convex (top right panel). These effects, however, are of second order relative to the increase in the mean-variance component of the stock demand. When r_0 increases, the IR hedge becomes more positive, while the MPR hedge exhibits little variation. Combining these two effects increases total hedging and stock demands. For typical values of the MPR (between 0 and 40 percent) and moderate IR levels (in excess of two percent), the positive IRH overwhelms the negative MPRH and the total hedging demand is positive.

B.2. Market Timing Strategies: Volatility and Lifecycle Effects

To assess the importance and stability over time of the hedging demands, we perform two market timing experiments. The first consists of drawing trajectories of the underlying state variables and computing the portfolio components along these trajectories. The second experiment simulates the optimal portfolio for very long horizons using actual market data.

Results for the first experiment are reported in Figure 4. A typical trajectory of the pair (r, θ) is drawn in the top panels. The IR varies between 5.4 percent and 6.3 percent; the MPR takes values between 0.02 and 0.20. The bottom left panel illustrates the stock demand and the MV component behaviors for an investor with risk aversion of 4 and a fixed horizon of five years. For the trajectory drawn, the proportion invested in the stock evolves between four percent and 28 percent. Close inspection of the graph, however, shows that changes superior to 20 percent in the portfolio share are usually spread over periods of six months or more.

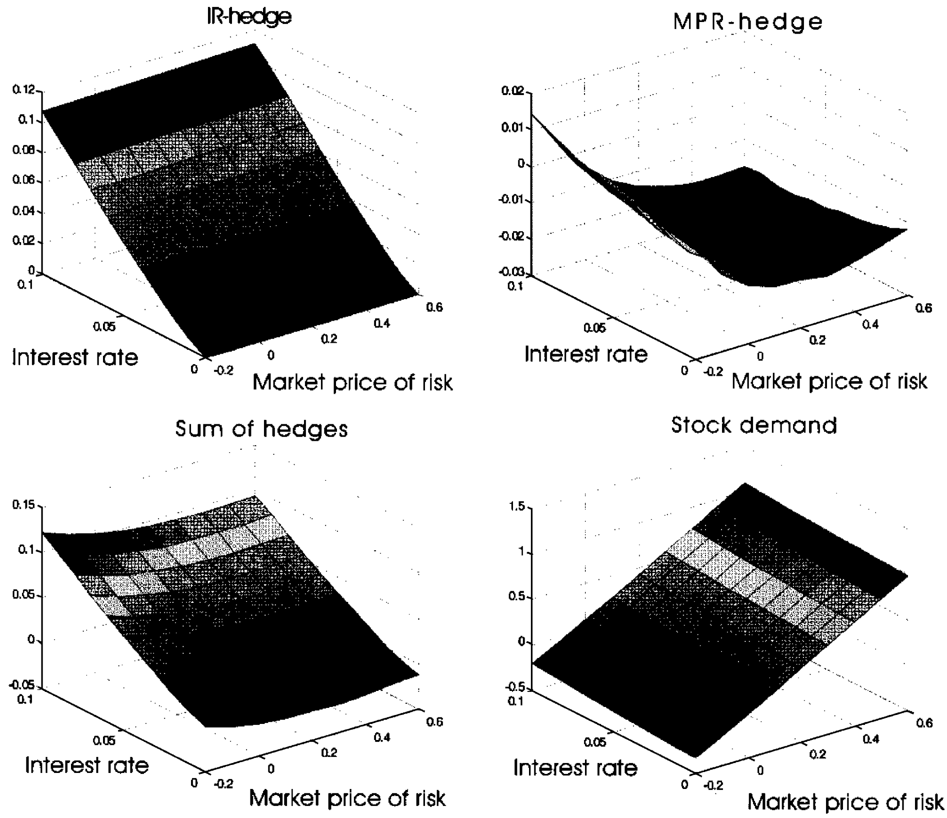

Figure 3. Effects of r_0 (initial level of interest rate) and θ_0 (initial level of market price of risk) on hedging demands and total demand for stocks when $r_0 \in [0, 10$ percent] and $\theta_0 \in [-0.2, 0.6]$.

There are also long stretches of time, in excess of a year, over which the stock share varies within a 10 percent interval.

The bottom right panel, which shows the respective contributions of the IR hedge, the MPR hedge and the sum of the two hedges, sheds further light on this issue. First note that the IR- hedge is remarkably stable over time. It experiences very small fluctuations and decreases slowly toward zero due to the maturity effect of the fixed horizon; it also remains positive throughout the period. The MPR hedge is negative and exhibits stronger volatility, which is not surprising since it is sensitive to the MPR level, which is more volatile. Within intervals of a year though, its fluctuations rarely exceed 10 percent. Again a trend toward zero is observed due to the fixed horizon. Both hedges work in opposite directions and partly offset each other. The net hedging correction is about 5.5 percent at the beginning of the investment horizon, thus boosting the stock demand. It then slowly converges toward zero while remaining positive. The net hedging correction inherits the stability of its components: its fluctuations rarely exceeds two

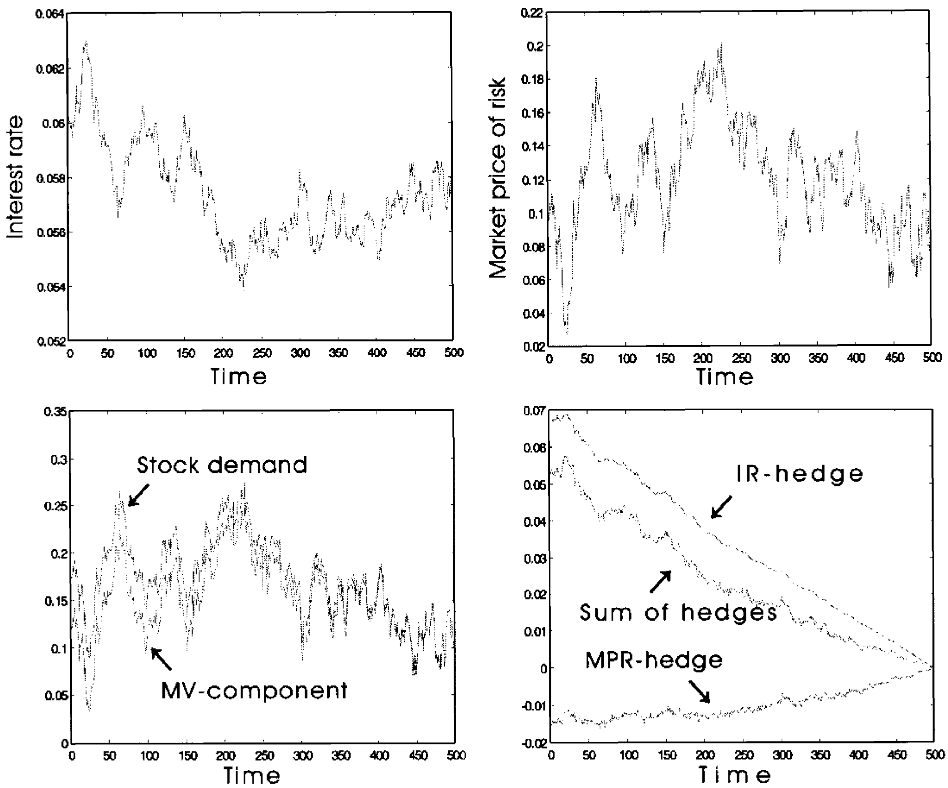

Figure 4. Market timing: hedging demands and total demand along trajectories of interest rate and market price of risk. Top panels plot typical trajectories of the IR and MPR processes. Bottom panels graph the fraction invested in the stock and the mean-variance demand (left) and the hedge components (right). $R = 4$; $T = 5$.

percent over periods of a year or longer. Over the whole five-year period, the net hedge varies between zero percent and six percent.

We conclude from this (representative) experiment that intertemporal hedges are remarkably stable over time in the sense that they exhibit low volatility. The variation in the total stock demand, which is observed in Figure 4, stems primarily from the variation of its mean variance component.

Our second experiment examines the actual behavior, based on market data, of the portfolio over time for an investor with long horizon of about 30 years at the beginning of the period. Hedging demands and portfolio positions are computed using our model along the realized trajectory of the IR and the MPR in the last 31.5 years (our estimation sample). Based on these data, we compute, for each month of the sample, the optimal share of the stock in the portfolio with and without hedging for an investor with a risk aversion of 4. As Figure 5 shows, intertemporal hedging increases the optimal share to a reasonable level of about 40 percent at the beginning of the investment horizon to roughly 5 percent at the end, with an average holding of 30 percent. This is in sharp contrast with the

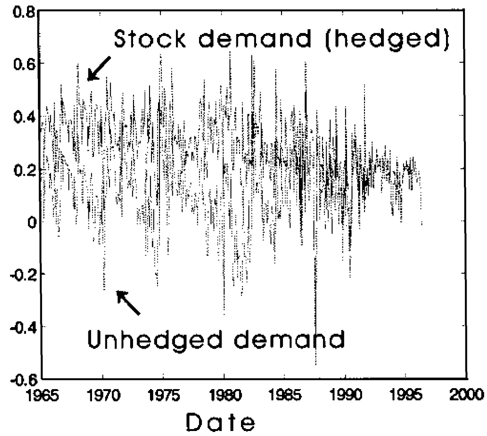

Figure 5. Market Timing: hedged and unhedged demands with actual data over a long horizon (1965 to 1996). Share of stock in portfolio with (top) and without (bottom) hedging. Fixed horizon of 31.5 years (our sample).

myopic mean-variance optimal share, which varies substantially around an average level of about 10 percent. Note also that the hedging investor will short the stock only six times during the investment period compared to 73 times for an unhedged investor. Naturally, the observed increase in stock holdings comes from the positive IR hedge. From this realistic situation, we also conclude that intertemporal hedging has a fundamental impact when the investment horizon is long. As in the previous experiment, it tends to stabilize the overall stock demand.

B.3. Stochastic Dividends

In the last decade, substantial evidence has accumulated to suggest that the dividend–price ratio (DPR), denoted by p, is a relevant factor which influences the evolution of the MPR. A natural question is whether the statistical relevance of the DPR translates into a significant impact on the portfolio allocation.

To examine this issue, we consider a generalization of our benchmark model in which the triplet (r, θ, p) satisfies

$$dr_t = \mu_r(r_t)dt - \sigma_r r_t^{\gamma_r} dW_t, \quad r_0 \text{ given} \tag{28}$$

$$d\theta_t = [\mu_\theta(\theta_t) + \mu_\theta^r(r_t, \theta_t) + \mu_\theta^p(p_t, \theta_t)]dt + \sigma_\theta(\theta_t)dW_t, \quad \theta_0 \text{ given} \tag{29}$$

$$dp_t = \mu_p(p_t)dt - \sigma_p p_t^{\gamma_p} dW_t, \quad r_0 \text{ given}, \tag{30}$$

where

$$\mu_\theta^p(p_t, \theta_t) \equiv \delta_p(\bar{p} - p_t)(\theta_l + \theta_t)\left(1 - \left(\frac{\theta_l + \theta_t}{\theta_l + \theta_u}\right)\right) \tag{31}$$

Table III

Dividend Effect—Portfolio Composition with Dividend Predictability

This table reports the optimal share of the portfolio invested in the stock (π), the interest rate hedge (IRH), and the market price of risk hedge (MPRH) for different risk aversions (R) and horizons (T). Computations are performed in the trivariate model with IR, MPR, and DPR (dividend–price ratio) state variables and three sources of uncertainty. The IR process is mean reverting with constant elasticity of variance (CEV) and exhibits nonlinearities in the speed of mean reversion. The MPR process exhibits mean reversion with hyperbolic elasticity of variance and interest rate dependence in the drift. The DPR follows a nonlinear mean-reverting CEV process and has a linear effect on the drift of the MPR. The values of the parameters for the processes are reported in Appendix C. For $R = 1$, the portfolio composition is the same as in Table II.

R		T					
		1	2	3	4	5	10
0.5	π	1.0437	1.0549	1.0530	1.0450	1.0364	0.9749
	MV	1.0000	1.0000	1.0000	1.0000	1.0000	1.0000
	IRH	– 0.0183	– 0.0364	– 0.0542	– 0.0719	– 0.0895	– 0.1753
	MPRH	0.0619	0.0912	0.1072	0.1170	0.1259	0.1502
2	π	0.2523	0.2577	0.2651	0.2720	0.2806	0.3189
	MV	0.2500	0.2500	0.2500	0.2500	0.2500	0.2500
	IRH	0.0092	0.0184	0.0276	0.0367	0.0459	0.0914
	MPRH	– 0.0069	– 0.0106	– 0.0125	– 0.0147	– 0.0152	– 0.0226
4	π	0.1332	0.1438	0.1558	0.1674	0.1799	0.2370
	MV	0.1250	0.1250	0.1250	0.1250	0.1250	0.1250
	IRH	0.0138	0.0276	0.0414	0.0552	0.0690	0.1378
	MPRH	– 0.0056	– 0.0087	– 0.0106	– 0.0128	– 0.0141	– 0.0257

$$\mu_p(p_t) = \kappa_p(\bar{p} - p_t)(1 + \phi_p(\bar{p} - p_t)^{2\eta_p}), \tag{32}$$

and $\mu_r(r_t)$ is also given by the function (32) substituting r for p.

In this specification, the DPR follows a nonlinear mean-reverting CEV process and has a linear effect on the drift of the MPR. In other respects, the IR and MPR processes are the same as in the benchmark case. To calibrate the model with stochastic dividends, we follow the same approach as for the benchmark case. The parameter values are in Appendix C. It should be noted that the calibrated parameters show strong effects of the IR and DPR on the drift of the MPR. All the other parameters remain close to the values obtained for the benchmark model with two state variables only.

Table III displays the optimal portfolio when stochastic dividends are accounted for. Strikingly, dividends appear to have very little effect on the portfolio composition over the range of risk aversions and horizons considered (compare with Table II). The intuition for this result stems from the fact that DPR does not have a direct effect on the state price density and optimal terminal consumption. Instead, it has an indirect effect through the drift of the MPR process, which implies a second order effect on the state price density and optimal consumption. The negligible effect of stochastic dividends stands in contrast with Barberis (2000), who found a strong effect of predictability through the DPR on the portfolio policy. Note, however, that his reference model had i.i.d. excess returns. As a result, adding the dividend yield as a predictor led to a considerable increase in predictive power and had a significant impact on the portfolio shares. In our benchmark model, predictability is already included through mean reversion and through the IR, which is a strong predictor of excess returns and the MPR. The additional predictive power of the dividend yield is, therefore, not as strong as in Barberis (2000).

B.4. The Importance of Modeling Nonlinearities

One important question concerns the relevance of a nonlinear process, such as the NMRHEV model, for asset allocation purposes. Even if this model provides a better empirical description of the data, it is by no means assured that portfolio rules will be significantly affected by the nonlinearities present in the data.

To address this issue, we examine the properties of the optimal portfolio obtained in each of the models. On one hand, we consider the NMRCEV–NMRHEVID model, described above, calibrated to the data. On the other hand, we examine a model in which the IR process is mean reverting with square-root volatility (MRSR) and the MPR follows a mean-reverting Gaussian process with a linear interest rate dependence in the drift (MRGID). Specifically, our second model is

$$dr_t = \kappa_r(\bar{r} - r_t)dt - \sigma_r r_t^{0.5} dW_t \tag{33}$$

$$d\theta_t = \big(\kappa_\theta(\bar{\theta} - \theta_t) + \delta_r(\bar{r} - r_t)\big)dt + \sigma_\theta dW_t, \tag{34}$$

where κ_r, $\bar{r}$, σ_r and κ_θ, $\bar{\theta}$, δ_r, σ_θ are nonnegative constants. Clearly, the MRSR–MRGID model is a subcase of our general setting obtained by setting some parameters equal to zero. Model parameters are calibrated to the data using the approach in Appendix C. Parameter values are reported in the same appendix.

The absence of a nonlinear term in the drift of the IR implies that we underestimate the speed of mean reversion in periods of high interest rates. This nonlinear term captures the faster mean reversion when the IR becomes large, as was the case at the beginning of the 1980s. Without this term, the mean reversion is as slow in periods of high and low interest rates, and this tends to increase the demand for the risky asset due to hedging considerations.

As for the MPR, a linear and constant diffusion coefficient leads to an underestimation of the corresponding hedging term. The volatility of the MPR is time varying and evolves in a nonlinear fashion. It is shown here that modeling this nonlinear behavior is important for the optimal portfolio.

Figure 6 displays the risk aversion effects for a fixed horizon of five years. The top panels show that the MRSR–MRGID specification overestimates (underestimates) the IR hedge and underestimates (overestimates) the MPR hedge when risk aversion exceeds (falls below) 1. The overall hedging demand and the total demand for the risky asset are always biased high. This follows since the IR hedge dominates when $R > 1$, while the MPR hedge tends to dominate when $R < 1$. The

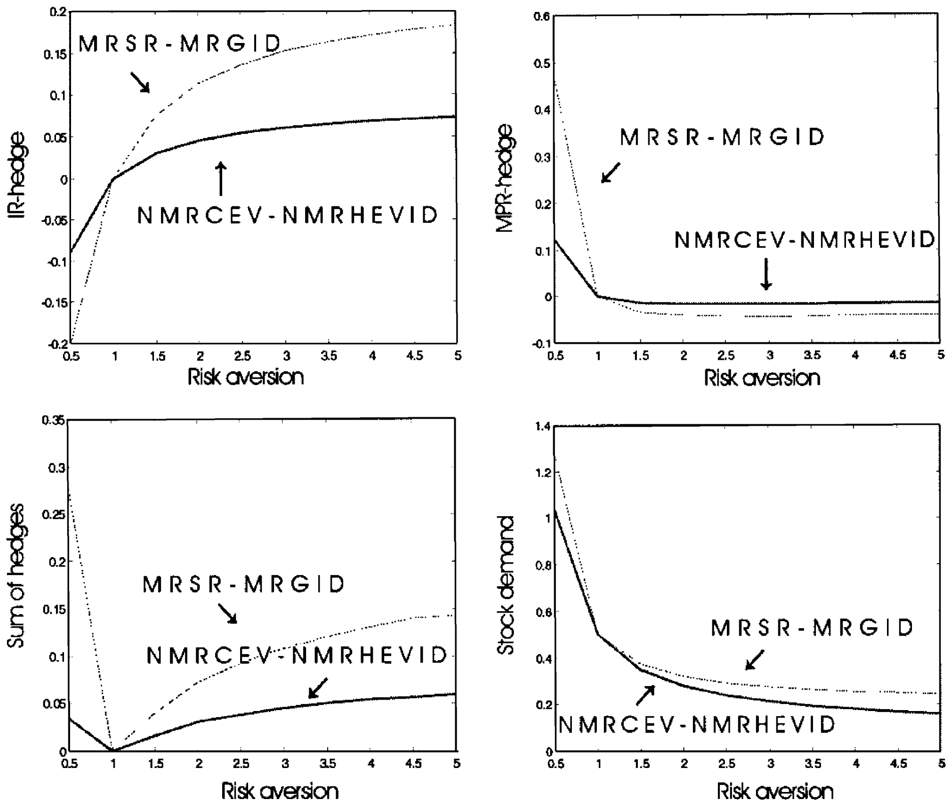

Figure 6. The effects of nonlinearities on total stock demand and hedging demands. IRH (top-left), MPRH (top-right), hedging demand (bottom-left) and total demand (bottom-right).

magnitude of the bias is important. For a risk aversion of 4, the optimal investment in the risky asset is overstated by about 42.67 percent (25.58 percent instead of 17.93 percent), the IRH by a factor of 2.5 (17.10 percent instead of 6.84 percent), and the MPRH is *under*stated by a factor of nearly 3 (− 4.02 percent instead of − 1.41 percent). Although not reported here, we have also examined the behavior of the bias as a function of the investment horizon. Our experiments have shown that the size of the bias increases with horizon.

V. Hyperbolic Absolute Risk Aversion (HARA Utility)

Utilities with constant relative risk aversion have become a central feature of the workhorse models in finance. Their appeal is partly based on the fact that the demand functions are proportional to wealth (see Merton (1971)), which improves the tractability of asset pricing or asset allocation models. From an economic perspective though, it is apparent that this property is very strong and unlikely to provide a good description of individual behavior. Some prominent economists (e.g., Arrow (1975)) have, in fact, argued that increasing relative risk aversion is a more compelling assumption. Others have suggested that the preservation of a minimum standard of living is a fundamental concern.

Utility functions in the HARA class can be used to model these aspects. They take the form

$$u(X) = \frac{1}{1-R}(X+B)^{1-R}, \tag{35}$$

where $R > 0$ and B are constants. The relative and absolute risk aversion coefficients are, respectively, $R(X) = RX/(X+B)$ and $R^a(X) = R/(X+B)$. Absolute risk aversion is decreasing and convex with an asymptote at $X = -B$. When $B > 0$, relative risk aversion is strictly increasing and concave, with an asymptote at $X = -B$. When $B < 0$, relative risk aversion is decreasing and convex in wealth and becomes infinite as wealth approaches the subsistence level $-B$.[15] In this case, the utility function displays intolerance for wealth levels below the floor $-B$. This specification is well suited to analyze portfolio allocation when a minimum terminal balance is sought. Portfolio insurance, goal constraints, and subsistence constraints are examples of problems in this category.

A. Binding Nonnegative Wealth Constraint

Although more compelling from an economic point of view, the generalized power utility has not seen much use because of its lack of tractability. One difficulty, highlighted by Cox and Huang (1989), is that consumption is nonlinear with respect to wealth at sufficiently low wealth. This is a consequence of the consumption constraint, which binds with positive probability and modifies the nature of the solution in a critical way. While Cox and Huang solve for the consumption policy in this setting, their analysis provides only limited information about the optimal portfolio. This is where our approach can prove useful, since it is ideally suited to study cases where nonlinearities matter.

The optimal portfolio is now given by (7)–(10) with $R(X) = RX/(X+B)$. Table IV reports the portfolio components, for a set of values of X and R, when the nonnegativity constraint on terminal wealth is accounted for and in the absence of a wealth constraint. Computations are performed for the three-state variables model with DPR effect of Section IV.B.3.

The table shows that the constraint has a dominant effect at low levels of wealth. In the absence of a constraint, the fraction invested in the stock, as well as the mean variance and hedging terms, explode. With a nonnegativity constraint, the behavior is much more reasonable. For instance, with $R = 1$, the IR hedge increases from -50.25 percent when wealth is 10 to -55.51 percent when wealth falls to 1. The corresponding numbers in the absence of the constraint are, respectively, -102.65 percent and -1027.16 percent! These results underscore the importance of accounting for wealth constraints for sound asset allocation rules.

[15] To ensure that preferences are defined for all $X \geq 0$, we set $u(X+B) = -\infty$ for $X < -B$, when $B < 0$.

Table IV

HARA Utility—Portfolio Components with a Wealth Constraint ($B = 100$)

This tables reports the optimal portfolio components: the total share π invested in the stock, the shares represented by the mean-variance (MV) component, the interest rate hedge (IRH), and the market price of risk hedge (MPRH). The utility function is of the HARA type, with relative risk aversion coefficient $R(X) = RX/(X+B)$. The shares are reported for a set of values of wealth (X) and risk aversion (R), when the nonnegativity constraint on terminal wealth is accounted for and in the absence of a wealth constraint. Computations are performed in the trivariate model with IR, MPR, and DPR state variables, and three sources of uncertainty. The IR process is mean reverting with constant elasticity of variance (CEV) and exhibits nonlinearities in the speed of mean reversion. The MPR process exhibits mean reversion with hyperbolic elasticity of variance and interest rate dependence in the drift. The DPR follows a nonlinear mean-reverting CEV process and has a linear effect on the drift of the MPR. The values of the parameters for the processes are reported in Appendix C.

R		X							
		1		5		10		100	
	constraint	with	without	with	without	with	without	with	without
1	π	2.7723	18.4078	2.0739	4.0807	1.7417	2.2853	0.6793	0.6793
	MV	2.1378	27.6850	1.9535	5.9346	1.8741	3.2163	0.7722	0.7722
	IRH	− 0.5551	− 10.2716	− 0.5182	− 2.0536	− 0.5027	− 1.0265	− 0.1029	− 0.1029
	MPRH	1.1896	0.9944	0.6386	0.1998	0.3704	0.0955	0.0099	0.0099
2	π	2.3485	8.6882	1.5648	1.9872	1.1324	1.1545	0.4066	0.4066
	MV	2.0322	13.8879	1.8145	2.9693	1.5144	1.6084	0.3860	0.3861
	IRH	− 0.5356	− 5.0905	− 0.4875	− 0.9400	− 0.3854	− 0.4227	0.0421	0.0421
	MPRH	0.8519	− 0.1093	0.2379	− 0.0420	0.0034	− 0.0312	− 0.0216	− 0.0216
4	π	1.9746	4.2165	1.0366	1.0469	0.6460	0.6461	0.2846	0.2846
	MV	1.9201	6.9059	1.4324	1.4853	0.8051	0.8051	0.1930	0.1930
	IRH	− 0.5100	− 2.4456	− 0.3564	− 0.3774	− 0.1180	− 0.1180	0.1153	0.1153
	MPRH	0.5645	− 0.2438	− 0.0393	− 0.0609	− 0.0410	− 0.0410	− 0.0237	− 0.0237

Perhaps more striking is the change in the signs of the hedges as wealth becomes low or as the coefficient R approaches one. To understand this property, suppose a unit increase in the state price density ξ_T and consider its impact on the cost of optimal consumption in a given state, $\xi_T((y\xi_T)^{-1/R} - B)^+$. Taking the derivative with respect to ξ_T shows that the marginal cost of consumption is positive (negative) if and only if

$$\left((y\xi_T)^{-1/R} - B\right)^+ - \frac{1}{R}(y\xi_T)^{-1/R}1_{X_T>0} = \left[\left(1-\frac{1}{R}\right)(y\xi_T)^{-1/R} - B\right]1_{X_T>0} \quad (36)$$

is positive (negative). The first term, $((y\xi_T)^{-1/R} - B)^+$, is the additional cost of maintaining consumption (income effect); the second term, $-(1/R)(y\xi_T)^{-1/R}1_{X_T>0}$, is the cost reduction induced by the response of optimal consumption (substitution effect). When $B = 0$ (i.e., CRRA), the net effect is driven by whether risk aversion exceeds, or falls below, 1. This was the case studied in the previous section. Suppose now $B > 0$. When initial wealth is low, this marginal cost is dominated by the negative substitution effect. At large values of wealth, and when $R > 1$, the positive income effect dominates. When R approaches 1, and for all values of wealth,

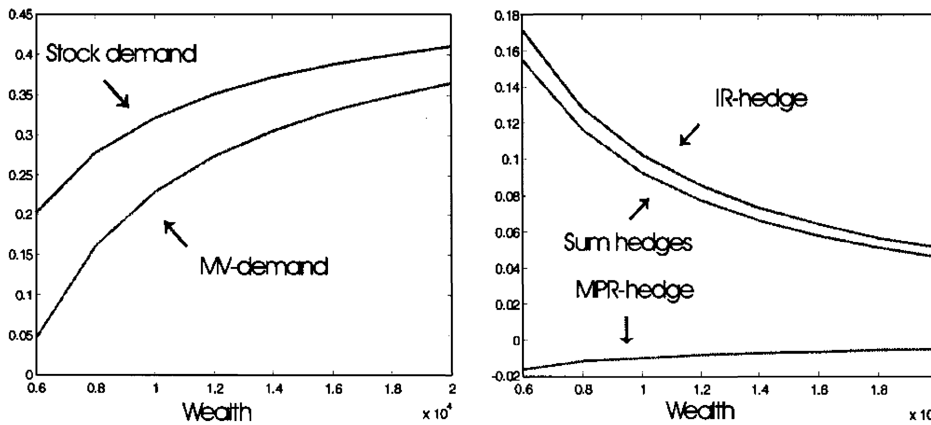

Figure 7. Intolerance for wealth shortfalls (portfolio insurance). Portfolio composition with a HARA utility function, $u(X) = (1/(1-R))(X+B)^{1-R}$, with $B = -10{,}000$, $R = 1$, and $T = 10$. Share in stock and MV component (left panel), IRH, MPRH, and sum of the hedges (right panel).

the net effect is negative. Since the investor, ultimately, seeks insurance against the impact of shocks on the cost of optimal consumption, it is clear that the relative strength of the two effects determines the signs of the hedges. In particular, as wealth decreases to 0 or R decreases to 1, we expect to see the IRH switching from positive to negative and the MPRH from negative to positive. This is precisely the behavior displayed in the table.[16]

Lastly, when wealth increases, the portfolio structure converges to that under constant relative risk aversion. This reflects the vanishing likelihood of a binding constraint. In the limit, the preference ordering of random terminal wealth is unaffected by the constant B.

B. *Intolerance for Wealth Shortfalls (Portfolio Insurance)*

When $B < 0$, preferences display intolerance for terminal wealth outcomes below the benchmark $-B$. The presence of this floor will induce a modification in the portfolio behavior as the investor seeks insurance against intolerable outcomes.

Figure 7 displays results for the three-state variables model with DPR effects and $R = 1$. The fraction invested in the stock market, the mean-variance (MV) component, and the MPRH are increasing functions of wealth, while the IRH is decreasing in wealth. As wealth approaches the present value of the floor, the investor adopts a more conservative policy: The fraction invested in the stock decreases to a positive value. This behavior may seem puzzling, since the MV

[16] When wealth is unconstrained, B has a marginal effect on the MPRH, since $\int_t^T \mathcal{D}_t\theta_s(dW_s + \theta_s ds)$ is a martingale under the risk neutral measure. The sign of the MPRH is then driven by the first term in the marginal cost of consumption, provided R is large enough. This explains the negative MPRH in Table IV at low wealth and $R = 2, 4$.

component vanishes (recall that the MV demand is inversely related to relative risk aversion which approaches infinity). The explanation lies in the behavior of the hedges. Even at low levels of wealth, the investor still cares about the present value of the floor and will seek to hedge against its fluctuations. This motivates hedging demands against the impact of IR and MPR innovations on the present value of the floor. In effect, the limiting portfolio synthesizes the floor $-B$ at date T.

At the other extreme, for large values of wealth, the floor becomes less relevant. In the limit, the investor behaves as if relative risk aversion were constant, and all the portfolio components converge to those of the limiting CRRA portfolio. With $R = 1$, the hedging terms eventually vanish.

VI. Investing in a Multiasset World

This section is devoted to large-scale models with multiple assets and state variables. We first outline the setting, then examine a particularly relevant model with old and new economy stock funds.

A. A Large-scale Model with Nonlinear Dynamics

Suppose that there are d Brownian motions and $d+1$ securities: $d-1$ stock portfolios, one mutual fund composed of long term pure discount bonds, and the riskless asset. There are $2d$ state variables: one interest rate, d market prices of risk, and $d-1$ state variables (dividends) affecting the evolution of the market prices of stock risks.

The dynamics of the interest rate (r) and the price of the bond portfolio (S_b) are

$$dr_t = \mu_r(r_t)dt - \sigma_r r_t^{\gamma_r} dW_{1t} \tag{37}$$

$$dS_{bt} = S_{bt}[(r_t + \sigma_b \theta_{1t})dt + \sigma_b dW_{1t}], \tag{38}$$

where $\mu_r(r_t)$ is given by (32) substituting r for p. Stock portfolios' prices (S_1, …, S_{d-1}) satisfy

$$\begin{aligned} dS_{it} + S_{it}p_{it}dt =& S_{it}\left(r_t + \sigma_i\left(\rho_{i,1}\theta_{1t} + \ldots + \rho_{i,i}\theta_{it} + \sqrt{1-\rho_i^2}\theta_{i+1t}\right)\right)dt \\ &+ S_{it}\sigma_i\left(\rho_{i,1}dW_{1,t} + \ldots + \rho_{i,i}dW_{i,t} + \sqrt{1-\rho_i^2}dW_{i+1,t}\right) \end{aligned} \tag{39}$$

for $i = 1, \ldots, d-1$, with $\rho_i^2 = \sum_{k=1}^{i} \rho_{i,k}^2$. The constant $-\rho_{i,1}$ is the correlation between IR changes and the return on fund i. The correlation between funds i and j, $i<j$, is $\rho_{i,1}\rho_{j,1} + \ldots + \rho_{i,i}\rho_{j,i} + \sqrt{1-\rho_i^2}\rho_{j,i+1}$. The coefficients σ_i, $\rho_{i,k}$ with $i, k = 1, \ldots, d-1$, are constant.

In this setting, W_1 is IR risk and $W_2, \ldots, W_d$ represent risk factors affecting stock returns. More specifically, W_2 captures the incremental risks affecting fund 1 after accounting for IR risk (i.e., fund 1 returns depend on (W_1, W_2)). Similarly, W_{k+1} is the incremental factor impacting the returns on fund k after the first k factors have been accounted for (i.e., fund k returns depend on ($W_1, \ldots, W_{k+1}$)).

Since there are $d+1$ securities and d Brownian motions, all risks can be hedged away. The bond portfolio provides a perfect hedge against IR risk.

To compute the optimal portfolio shares, we assume that (θ, p) follow a joint diffusion process, which satisfies the assumptions of Theorem 1. The structure of the optimal portfolio is intuitive. First, note that fund $d-1$ is the only one exposed to W_d risk. Since other sources of risk (i.e., $W_1,\ldots,W_{d-1}$), can be hedged away, the demand for fund $d-1$ is entirely driven by the risk-return characteristics associated with W_d. Therefore, the demand for fund $d-1$,

$$\pi_{d-1,t} = \frac{1}{\sigma_{d-1}\sqrt{1-\rho_{d-1}^2}}\left[\frac{1}{R}\theta_{dt} - \bar{a}_d(r_t, \theta_t, p_t)\right] \tag{40}$$

includes a mean-variance component and an intertemporal hedge against fluctuations in the opportunity set induced by W_d risk (term involving $\bar{a}_d(r_t, \theta_t, p_t)$). In effect, fund $d-1$ provides the best hedge against this particular source of risk.

However, the structure of the portfolio shares for the other funds is different. Indeed, since the returns on fund $d-1$ also depend on $W_1, \ldots, W_{d-1}$, the position taken in fund $d-1$ induces an exposure to W_k equal to $\sigma_{d-1}\rho_{d-1,k}\pi_{d-1,t}$ for $k=1, \ldots, d-1$. The investor uses the other funds to hedge these induced exposures away. For example, fund $d-2$ serves to eliminate the exposure to W_{d-1} risk, $\sigma_{d-1}\rho_{d-1,d-1}\pi_{d-1,t}$. Its demand is given by

$$\pi_{d-2,t} = \frac{1}{\sigma_{d-2}\sqrt{1-\rho_{d-2}^2}}\left[\frac{1}{R}\theta_{d-1t} - \bar{a}_{d-1}(r_t, \theta_t, p_t)\right] - \frac{\sigma_{d-1}\rho_{d-1,d-1}}{\sigma_{d-2}\sqrt{1-\rho_{d-2}^2}}\pi_{d-1,t}. \tag{41}$$

This explains the last component in $\pi_{d-2,t}$. The remaining demand for fund $d-2$ has the usual structure, namely a mean-variance term and an intertemporal hedge against fluctuations induced by W_{d-1} risk (term with $\bar{a}_{d-1}(r_t, \theta_t, p_t)$). Similarly, fund k serves to hedge away the exposure to W_{k+1} risk induced by the demands for funds $k+1,\ldots,d-1$. The remaining demand components are the mean-variance term and an intertemporal hedge against W_{k+1} risk. This structure is common to all funds' demands, including the bond fund, which is given by,

$$\pi_{b,t} = \frac{1}{\sigma_b}\left[\frac{1}{R}\theta_{1t} - \bar{a}_1(r_t, \theta_t, p_t)\right] - \frac{1}{\sigma_b}\left(\sum_{j=1}^{d-1}\sigma_j\rho_{j,1}\pi_{j,t}\right). \tag{42}$$

In these expressions, $\bar{a}_i(r_t, \theta_t, p_t) = a_i(r_t, \theta_t, p_t) + b_i(r_t, \theta_t, p_t)$ where $a_i(r_t, \theta_t, p_t)$, $b_i(r_t, \theta_t, p_t)$ are defined in Section 3.

To demonstrate the versatility of the approach, we take 11 assets, 20 state variables, and 10 sources of uncertainty ($d=10$). The first fund is the market portfolio of risky securities (its returns depend on (W_1, W_2)). The next eight funds are pure hedging funds: We assume that fund j is perfectly correlated with W_{j+1} risk, $j=2,\ldots,9$ (i.e., $\rho_{j,k}=0$ for $k \leq j$). The bond fund hedges W_1 risk. We also assume a symmetric structure for the state variables θ, p: For $i=2,\ldots,d$, each pair (θ_i, p_i) satisfies an identical NMRHEV–NMRCEV process as in the benchmark model with DPR; for $i=1$ the market price of IR risk satisfies an NMRHEV process

Table V

Stock, Bond, and Mutual Fund Demands in the Multiasset Model

This table reports the optimal shares invested in the stock market index (π_s), a long-term bond fund (π_b), and a mutual fund (π_2), in a model with 11 assets (10 risky assets and cash), 20 state variables, and 10 sources of uncertainty. The state variables are the interest rate (IR), 10 market prices of risk (MPR), and 9 dividend-price ratios (DPR). A symmetric structure is assumed: Each pair of state variables (MPR, DPR) follows an identical bivariate process with nonlinear mean reversion and hyperbolic elasticity of variance for the MPR and nonlinear mean reversion with constant elasticity of variance for the DPR. The market price of IR risk satisfies a nonlinear mean-reverting process with constant elasticity of variance and without dividend effect. For parameter values, we took the estimates in the corresponding benchmark models. The table displays the portfolio behavior when risk aversion and the correlation coefficient ρ_1 between the IR and the stock market index vary.

R		correlation				
		– 0.9000	– 0.5000	0.0000	0.5000	0.9000
1	π_s	1.1470	0.5773	0.5000	0.5773	1.1470
	π_b	1.5323	0.7886	0.5000	0.2113	– 0.5323
	π_2	0.5000	0.5000	0.5000	0.5000	0.5000
2	π_s	0.5341	0.2707	0.2345	0.2718	0.5353
	π_b	0.8062	0.4611	0.3252	0.1906	– 0.1562
	π_2	0.2338	0.2342	0.2339	0.2333	0.2343
3	π_s	0.3496	0.1762	0.1533	0.1770	0.3453
	π_b	0.5832	0.3565	0.2673	0.1788	– 0.0419
	π_2	0.1517	0.1529	0.1537	0.1539	0.1522
4	π_s	0.2648	0.1289	0.1124	0.1298	0.2578
	π_b	0.4780	0.3051	0.2386	0.1755	0.0036
	π_2	0.1164	0.1153	0.1144	0.1140	0.1149

without dividend effect. For parameter values, we took the estimates in the corresponding benchmark models (with DPR for $i = 2,\ldots,d$ and without for $i = 1$).

Table V displays the portfolio behavior when risk aversion and the correlation coefficient ρ_1 between the IR and the stock market index vary. Note that the demand for the stock is convex with respect to correlation. This reflects the particular risk-return trade-off embedded in the demand for the market portfolio (inversely related to the stock's exposure to pure market risk, $\sigma_1\sqrt{1-\rho_1^2}$). The demand is maximal when the correlation approaches ± 1: In the limit, the investor attempts to extract benefits from the stock's vanishing exposure to W_2 and can only do so by increasing the scale of his holdings in an unbounded manner. Naturally, this behavior is strongest at lower levels of risk aversion.

The bond fund hedges against IR risk. When the demand for the market portfolio increases, the exposure of the portfolio to IR risk increases as well, and this prompts an increased demand for fund 1. With negative (positive) correlation, this entails taking a positive (negative) position in the bond fund. Again, demand explodes as correlation approaches ± 1, reflecting the behavior of the stock demand. Other funds are held for risk-return trade-off as well as hedging purposes. Since funds' risks do not affect the IR or the market price of stock market risk in this model, these hedging demands serve the sole purpose of hedging MPR fluctuations.

B. Asset Allocation in the New Economy (Four Asset Classes)

We now specialize our multiasset model to four asset classes: three risky funds ($N = 3$) and cash (the riskless asset). The risky funds are a portfolio of "old-economy" stocks (S&P500), a portfolio of "new-economy" stocks (Nasdaq), and a portfolio of long-term pure discount bonds. Old-economy stocks are comprised of firms involved in traditional activities, such as manufacturing, industry, and services. They typically pay dividends. New-economy stocks are identified with communications, Internet, and biotechnology, among others. There are three Brownian motions, four securities, and five state variables (one IR, three MPRs, and one DPR) affecting the opportunity set.

The price of the bond portfolio S_b is given by (38). Old- and new-economy portfolios prices, S_1 and S_2, follow the dynamics (39) with $d = 3$. In this model, W_1 is an IR risk factor, W_2 is old-economy firms' risk, and W_3 represents new-economy risk factors. The IR r satisfies (37). The MPRs (θ_1, θ_2, θ_3) and the DPR of old-economy stocks p follow the correlated processes

$$d\theta_{it} = \left(\kappa_{\theta i}\left(\bar{\theta}_i - \theta_{it}\right) + \mu^r_{\theta i}(r_t, \theta_{it}) + \mu^p_{\theta i}(p_t, \theta_{it})\right)dt + \sigma_{\theta i}(\theta_{it})dW_t; \quad i = 1, 2, 3, \tag{43}$$

$$dp_t = \mu_p(p_t)dt - p_t^{\gamma_p}\sigma_p dW_t, \tag{44}$$

where $\mu^r_{\theta i}(r_t, \theta_{it})$ is defined in (25), $\mu^p_{\theta i}(r_t, \theta_{it})$ and $\mu_p(p_t)$ are as in (31) and (32), and $\sigma_{\theta i}(\theta_{it})$ is given by (26). In the expression for $\sigma_{\theta i}(\theta_{it})$, the term $\sigma_{\theta i} \equiv [\sigma_{i1}, \sigma_{i2}, \sigma_{i3}]$ is a 1×3 vector. The volatility of the DPR, $\sigma_p \equiv [\sigma_{p1}, \sigma_{p2}, \sigma_{p3}]$, is also 1×3. Thus, we allow for arbitrary correlations among MPRs and between the MPRs and the DPR.

The fractions of wealth invested in the stock funds (π_{1t}, π_{2t}) and the bond fund (π_{bt}) have the structures discussed in Section VI.A, and the same general comments apply. To get more insights about the portfolio properties, we calibrate the model (see Appendix C) and compute the investment shares. Table VI displays their behavior with respect to maturity when risk aversion equals 4. Two surprising properties are the negative holdings of long-term bonds and the decreasing fraction invested in stocks when the horizon increases. For instance, with a horizon of six years, 79 percent of wealth is in the S&P500, 11.7 percent in the Nasdaq, and -12.2 percent in the bond portfolio; with a 10-year horizon, the respective shares are 73.4 percent, 11.3 percent, and -12.4 percent. Moreover, the investor displays, in general, a preference for traditional "old-economy" stocks over more risky "new-economy" stocks.

The negative demand for long-term bonds is prompted by hedging considerations. While the mean-variance term and the intertemporal hedge are positive, they are overwhelmed by the hedging demand induced by investments in the S&P500 and the Nasdaq. For instance, with a horizon of six years, we have a mean-variance demand of 36.8 percent, an intertemporal hedge of 2 percent, and an induced hedge of -51 percent. The sign of the induced hedge follows from the negative association between interest rate risk and stock or bond returns. Given the positive investments in the S&P500 and the Nasdaq, the correlation structure prompts a position of the opposite sign in the bond portfolio. The size

Table VI

NASDAQ, S&P500, and Bond Demands

This table reports the optimal shares invested in the S&P500, the NASDAQ, and a bond fund, in a model with four asset classes and three sources of uncertainty. The demand for cash, the last asset, is 100 percent minus the sum of the other demands. The state variables are the interest rate (IR), the three market prices of risk (MPR) and the dividend price ratio of the S&P500 (DPR). The MPRs follow processes with nonlinear mean reversion and hyperbolic elasticity of variance. The DPR and the IR follow mean-reverting constant elasticity of variance processes, as in the benchmark model with DPR. The parameter values are reported in Appendix C. The table displays the portfolio behavior for a coefficient of relative risk aversion of 4 and maturities from 2 to 10 years.

		Maturity				
		2	4	6	8	10
SP500	Holding	0.8296	0.8221	0.7901	0.7652	0.7345
	MV	0.7332	0.7332	0.7332	0.7332	0.7332
	Intertemporal Hedge	0.0679	0.0643	0.0333	0.0100	− 0.0214
	Induced hedge	0.0284	0.0244	0.0234	0.0219	0.0226
NASDAQ	Holding	0.1411	0.1212	0.1166	0.1092	0.1127
	MV	0.1940	0.1940	0.1940	0.1940	0.1940
	Intertemporal hedge	− 0.0529	− 0.0728	− 0.0774	− 0.0848	− 0.0813
Long term	Holding	− 0.0648	− 0.0799	− 0.1220	− 0.1681	− 0.1239
Bonds	MV	0.3683	0.3683	0.3683	0.3683	0.3683
	Intertemporal hedge	0.1160	0.0831	0.0204	− 0.0442	− 0.0144
	Induced hedge	− 0.5493	− 0.5314	− 0.5109	− 0.4922	− 0.4779

of this hedging demand is prompted by the large fraction of wealth invested in the S&P500 and the Nasdaq.

The fact that the share invested in stocks goes down with the horizon goes against the popular notion that "stocks are less risky in the long run" and, therefore, should be held more prominently in longer horizon portfolios. This surprising conclusion reflects the congruence of several effects. First, note that the MPR hedge in the Nasdaq demand becomes more important (i.e., more negative) with the horizon. This horizon impact on the hedge is typical: It parallels the hedging behavior uncovered in the simpler models of prior sections. It contributes to a reduction in the investment in new economy stocks. Second, note that the intertemporal hedge component of the S&P500 demand displays more intricate effects. This hedge is positive for short horizons, but decreases and eventually becomes negative. The sign reversal is new in the context of models with constant relative risk aversion and reflects the conflicting effects of W_2 innovations on θ_1 and on (θ_2, θ_3) (i.e., $\sigma_{12} > 0$ and $\sigma_{22}, \sigma_{32} < 0$). The reduction of this hedge decreases the demand for the S&P500. Finally, note that the induced hedging component in the S&P500 demand decreases as well; this reflects the reduced exposure to old-economy risks induced by the decreasing fraction of wealth invested in the Nasdaq.

The Nasdaq demand is fueled by a positive mean-variance term (about 19 percent with a six-year horizon), which is reduced by an intertemporal hedge (about 8 percent). This hedging demand is entirely motivated by fluctuations in the market prices of risk θ due to Nasdaq risk W_3. The size of this MPR hedge illustrates the fact that MPR fluctuations are important in a multiasset world (the MPR hedge represents roughly -66 percent of the fraction held when $T=6$).

The demand for the S&P500 has an important mean-variance term and more modest hedging components. For a horizon of six years, the mean-variance term is 73.3 percent, the intertemporal hedge 3.3 percent, and the hedge induced by the position in the Nasdaq about 2.3 percent. Interestingly, the position in the Nasdaq prompts an increase in the demand for the S&P500. This is due to the negative correlation, $\rho_{2,2} = -0.1274$, between the Nasdaq and old-economy risk factor W_2. Equally surprising is the fact that the intertemporal MPR hedge increases the demand for the S&P500 (for horizons less than 10 years). This reflects, again, a correlation effect: Here, it is negative correlation between S&P500 risk factors (i.e., W_2) and their MPR (θ_2), which is a source of the result.

VII. A Comparison of Methods in the Benchmark Model

The Monte Carlo approach entails the computation of expectations that depend on the Malliavin derivatives of the state variables. In numerical implementations, the state variables and their Malliavin derivatives are simulated using the Euler scheme, with or without transformation of the state variables. An alternative approach, proposed by Brennan et al. (1997), computes the portfolio using the Bellman equation for the value function of the problem. In this section, we compare the two approaches and document the numerical advantages of our method. We perform this comparison in the benchmark model with CRRA.

A. Three Competing Methods

We consider three approaches. The first one is the Monte Carlo approach using Malliavin derivatives, which was described in Sections II and III. To simplify the notation, we refer to it by the acronym MCMD (Monte Carlo with Malliavin Derivatives).

The second is a PDE method based on the dynamic programming approach of Merton (1971). For CRRA, the proportions invested are independent of wealth and given by

$$\pi'\sigma = \frac{1}{R}\theta' + \frac{f_y}{f}\sigma^Y \tag{45}$$

$$\mathcal{L}f - \rho\theta'(f_y\sigma^Y)' + \left(\frac{1}{2}\rho(\rho-1)\|\theta\|^2 - \rho r\right)f = 0, \tag{46}$$

where $\rho = 1 - \frac{1}{R}$ and $f(T,\ \cdot) = 1$. This characterization of the portfolio, with a linear PDE for the function f, appears in Schroder and Skiadas (1999) and Liu (2001).[17] It simplifies the computational task and, therefore, biases the results in

[17] The approach in Brennan et al. (1997) is based on the nonlinear PDE for the function p, defined by $p \equiv \log f$.

favor of the PDE method. We take it as a basis for our comparison.[18] In the numerical implementation, the solution is computed using the method of Finite Differences. We refer to this combination by PDEFD (PDE Finite Differences).

The third approach is another Monte Carlo method recently proposed by Cvitanic et al. (CGZ) (2003). It uses the fact that the portfolio is the limit of the covariation[19]

$$\hat{\pi}_t'\sigma_t = \lim_{h\to 0} \frac{\mathbf{E}_t\left[\xi^{\rho}_{t,T}\frac{(W_{t+h}-W_t)}{\xi_{t,t+h}}\right]}{\mathbf{E}_t\left[\xi^{\rho}_{t,T}\right]}. \tag{47}$$

The procedure proposed by CGZ approximates the portfolio by fixing a discretization h. It then computes the conditional expectations on the right-hand side for this chosen h. The procedure appears easy to implement, since it does not involve Malliavin derivatives.[20] But it is based on an approximation (because h is fixed), and this will affect its convergence properties. We call this method MCC (Monte Carlo Covariation).[21]

[18] The link with Monte Carlo is easy to see, since the solution of (46) can be written as $f(t, Y_t) = \mathbf{E}_t[\xi^{\rho}_{t,T}]$. Taking the Malliavin derivatives on both sides of this equation gives $\mathcal{D}_t f(t, Y_t) = f_y(t, Y_t)\sigma^Y(t, Y_t) = -f(t, Y_t)(a(t, Y_t) + b(t, Y_t))$ and therefore $(f_y/f)\sigma^Y = -(a+b)$, where a, b are defined in (12) and (13). This shows that (45) and (7) are different representations of the same function.

[19] The optimal portfolio is the covariation between optimal wealth and the Brownian motion, $d[X, W]_t = \pi_t' X_t \sigma_t dt$. Thus, $\pi_t'\sigma_t = X_t^{-1}\lim_{h\to 0}\frac{1}{h}\mathbf{E}_t[(X_{t+h}-X_t)(W_{t+h}-W_t)] = \lim_{h\to 0}\frac{1}{h}\mathbf{E}_t[(X_{t+h}/X_t)(W_{t+h}-W_t)]$. Formula (47) follows since $X_{t+h}/X_t = (\mathbf{E}_{t+h}[\xi^{\rho}_{t,T}]/\mathbf{E}_t[\xi^{\rho}_{t,T}])\times\xi^{-1}_{t,t+h}$.

[20] The Monte Carlo Covariation method may be better suited to handle non-Markovian dynamics. However, it does not provide the IR- and MPR-hedge decomposition that MCMD provides.

[21] Brandt et al. (2001) propose another simulation method in discrete time. Their procedure involves three steps. The first step approximates the Bellman equation using a Taylor series expansion around wealth growing at the riskless rate (a quartic expansion is suggested by BGS). The optimal portfolio for this approximate problem satisfies a nonlinear polynomial equation (first-order condition) whose coefficients are expectations of the unknown value function and its derivatives. The second step uses a regression method in combination with Monte Carlo simulation to estimate these coefficients. This step parallels the algorithm proposed by Longstaff and Schwartz (2000) for the valuation of American-style options. The last step computes the approximate optimal portfolio using an iterative procedure to solve the nonlinear polynomial first-order condition. Since the estimate of the approximate portfolio at a given point in time requires knowledge of future estimates of the approximate portfolio, the algorithm is applied in a backward manner starting with the last period and moving recursively through time. The overall methodology is somewhat similar to CGZ, in that it provides a numerical estimation of an approximation of the optimal portfolio. Implementation raises challenging questions. First, for a fixed polynomial basis, the approximate solution will not converge to the true portfolio policy when the size of the time interval decreases, but to its projection on the selected basis (see Clément, Lamberton, and Protter (2002) for a proof of this result for American-style options). When the residual of this projection is large, the method cannot give a precise approximation. Second, proper implementation requires auxiliary tests to verify the optimality of the portfolio computed for the approximate problem. These tests are required because the approximate objective function (being a polynomial) need not be concave, and the first-order conditions (being polynomial equations) may have multiple

Table VII

Convergence Rates for Numerical Methods Used to Compute Portfolio Demands

The table compares the convergence rates of three numerical methods that are used to compute the optimal portfolio in the benchmark model with constant relative risk aversion. Convergence rates are expressed in terms of the discretization step (h), the number of discretization points in space or simulations (M), and the number of discretization points in time (N). The competing methods are the PDE (partial differential equations) finite difference methods, the Monte Carlo covariation method (MCC), and the Monte Carlo Malliavin derivatives method (MCMD). The table shows that the order of convergence for MCC and PDEFD depends on three terms, including a term of order h for MCC and $\min_j h_j^2$ for PDEFD. This term appears because these methods do not provide a numerical approximation of the true optimal portfolio, but rather a numerical approximation of an approximation of the true policy. This term is absent from MCMD because the true optimal portfolio is computed.

Estimator	Convergence rates
PDE finite difference methods (PDEFD)	
Explicit (PDEFD-E):	$O\left(\frac{1}{N} + \frac{1}{\max_j M_j^2} + \min_j h_j^2\right)$
Crank–Nicholson (PDEFD-CN):	$O\left(\frac{1}{N^2} + \frac{1}{\max_j M_j^2} + \min_j h_j^2\right)$
Monte Carlo covariation (MCC)	$O_P\left(\frac{1}{N} + \frac{1}{\sqrt{Mh}} + h\right)$
Monte Carlo Malliavin derivatives (MCMD)	$O_P\left(\frac{1}{N} + \frac{1}{\sqrt{M}}\right)$

B. Convergence Rate

Our first comparison between the three approaches involves their respective convergence properties, which are summarized in Table VII.

For PDEFD methods, the space is discretized in M_j points for state variable j and time in N points; the computation of numerical derivatives uses a discretization of length h_j for the derivative relative to j. For Monte Carlo methods, M is the number of replications and N the number of time points; for MCC, we also have h for the time increment used to compute the approximation in (47). The table shows that the order of convergence for MCC and PDEFD depends on three terms, one of order h for MCC and $\min_j h_j^2$ for PDEFD. This term appears because these methods do not provide a numerical approximation of the true optimal portfolio, but rather a numerical approximation of a convergent approximation of the true policy. This term is absent from MCMD, since the true optimal portfolio is computed.

In the case of MCC, this additional term slows down the overall convergence rate, since we draw random variables whose variance depends on the discretization parameter h. This perturbation parameter must then be controlled jointly

roots. These verifications could add substantial computation time to the procedure. In addition, for wealth-dependent utility functions, their method solves the problem for a grid of values for wealth. This introduces another approximation and increases the computation time.

with the choice of the number of Monte Carlo replications. Otherwise, the variance of the estimator will explode. In contrast, this term does not affect the overall convergence rate of PDEFD methods, since both implicit and explicit methods are already second order in space.

What about the other terms in the order of convergence? For PDEFD, these terms appear because discretization is in time (N) and space (M_j). For MC methods, we rely on a law of large numbers to approximate an expectation by an average over M replications. The second error is due to the fact that, in general, we cannot sample from the true distribution of $\xi_{t,\ T}$ but, instead, we must rely on a numerical solution of the SDE based on a discretization scheme.

The denominators of the expressions in Table VII show that PDE methods converge faster than MC methods. An important caveat is in order in that regard. PDE methods converge globally at the given rate if and only if the boundary conditions are correct. Unfortunately, the choice of appropriate boundary conditions is a nontrivial issue. If the domain of state variables is unbounded, in order to obtain a finite numerical algorithm, we must impose nonnatural boundaries and specify the unknown behavior of the function at those points. For example, if the short rate is unbounded, we must specify some upper bound r_u. Since $\xi_{t,T}$ decreases in r, it makes sense to impose an absorbing Dirichlet condition $f(\cdot,\ r_u,\ \cdot)=0$. Unfortunately, this could induce a discontinuity in the function and prevent attainability of the theoretical convergence rate.[22] Alternatively, if we impose a reflecting Newton boundary condition, say $\partial_r f(\cdot,\ r_u,\ \cdot)=0$, and if this condition is misspecified, we would not attain the theoretical convergence rate either.

The main difference between the two Monte Carlo methods comes from the order of convergence of the limiting distribution of the errors.[23] It is $\sqrt{M}/N$ for MCMD and $M^{1/3}/N$ for MCC. This means that if we want to shorten the length of asymptotic confidence intervals by half, we need only quadruple the number of replications and double the number of discretization points in time using MCMD. With MCC, we need eight times more replications and still must double the number of discretization points in time. Moreover, we must simultaneously shorten the time lead for the increment of the Brownian motion by half. If $1/h$ and/or N are increased at a higher rate, the asymptotic variance explodes and so does the length of asymptotic confidence intervals. On the other hand, if $1/h$ and/or N are increased at a lower rate, the second-order bias increases, which reduces the true coverage probability of confidence intervals based on the normal distribution with a given nominal size.

C. Efficiency

Another important aspect of the comparison is the efficiency of the method, which can be measured by the amount of memory required and the number of arithmetic calculations performed. The latter determines the speed of execution.

[22] See Heston and Zhou (2001) for more results along these lines.

[23] For full details and expressions for the limit distributions, see DGR (2001).

It is not the purpose of this paper to compare the methods in every detail. However, a few items are important to properly assess the candidates.

The computational requirements of the various methods are very different. For PDE methods, a better rate of convergence may not result in less CPU time. For example, the system matrix for Crank–Nicholson with three state variables needs about 640 megabytes of memory.[24] This requirement grows exponentially with the dimension of the problem and quickly becomes an impediment in a realistic portfolio problem with a large number of state variables. Explicit PDE methods require far less memory than implicit methods, but they run into a stability problem, since the discretized equations are sensitive to small errors.

With MC methods, the addition of a new state variable increases the number of operations required linearly, making them particularly suited for large multivariate problems. For MCMD, each state variable requires the simulation of a Malliavin derivative with respect to each Brownian motion. Since MCC does not require the simulation of any auxiliary process, it dominates in terms of computation time. Unfortunately, it converges at a slower rate than MCMD, and this worsens its efficiency properties.

The best way to gauge the relative performance of competing methods is to compare them in a concrete experiment. We will choose a relatively small-dimension problem in terms of state variables, making it harder for MC methods. On the other hand, we will compute a large number of portfolios, making it harder for PDE methods.

D. Experimental Setting and Numerical Results

We now illustrate the performance of the various methods for our benchmark model. We consider a mutual fund with 100 different types of clients who can be classified in 10 investment horizon classes (1 to 10 years) and 10 risk profiles (risk aversions from 0.5 to 5.5). For each method, we compute portfolio estimates for the 100 client configurations selected. Based on this empirical distribution, the sample root mean square relative errors (RMSE) and the maximal absolute errors (MAE) are recorded, and plotted against computation time. The experiment is repeated for different combinations of M, N, and h described below (we consider six combinations in the graphs). Errors are computed relative to a benchmark calculated using MCMD with 1,000 discretization points per year and 3,000,000 replications. All computations are for initial values close to the long-term means $\theta_0 = 0.1$, $r_0 = 0.06$, and $p_0 = 0.03$. The boundary conditions for the PDE methods are as follows. For the Explicit method, we simply impose $f(\cdot, 0.3) = 0$; for Crank–Nicholson, we require $f_r(\cdot, 0.3) = 0$, $f_r(\cdot, 0) = 0$, $f_p(\cdot, 0) = 0$, $f_{pp}(\cdot, 0.2) = 0$, $f_\theta(\cdot, -1.5) = 0$, and $f_{\theta\theta}(\cdot, 1.5) = 0$.

In the plots, N is the number of discretization points in time per year and M the number of replications (resp. discretization points in space) for Monte Carlo

[24] This storage requirement can be avoided if, at each time step, we rebuild the matrix system from scratch. But, doing so will considerably increase the computation time.

(resp. PDE) methods. The following legend applies:

$\diamondsuit^i$: Malliavin derivatives (MCMD): $N = 10 \times 2^{i-1}$ and $M = 1000 \times 2^{2(i-1)}$

$\times^i$: Covariation (MCC): $N = 10 \times 2^{i-1}$, $M = 100 \times 2^{3(i-1)}$, and $h = 0.1/2^{i-1}$

$+^i$: Explicit (PDEFD-E): $N = 10 \times 2^{i-1}$ and $M = h = [M_\theta, M_r, M_p] = 2 \times 2^i[1, 1, 1]$

$\bigcirc^i$: Crank–Nicholson (PDEFD-CN): $N = 2+i$ and $M = h = [M_\theta, M_r, M_p] = (2+i)[1, 1, 1]$.

Figure 8 shows that, among all methods, MCC does worst, whereas MCMD does best. This dominance occurs whether one uses MAE or RMSE for comparison. If we focus on MCC and MCMD, we see that the dominance of MCMD is systematic and significant. For the same budget of computation time, errors produced by MCC are larger by a factor of 10 or more. For the case $i = 5$, this factor reaches 100 for RMSE.

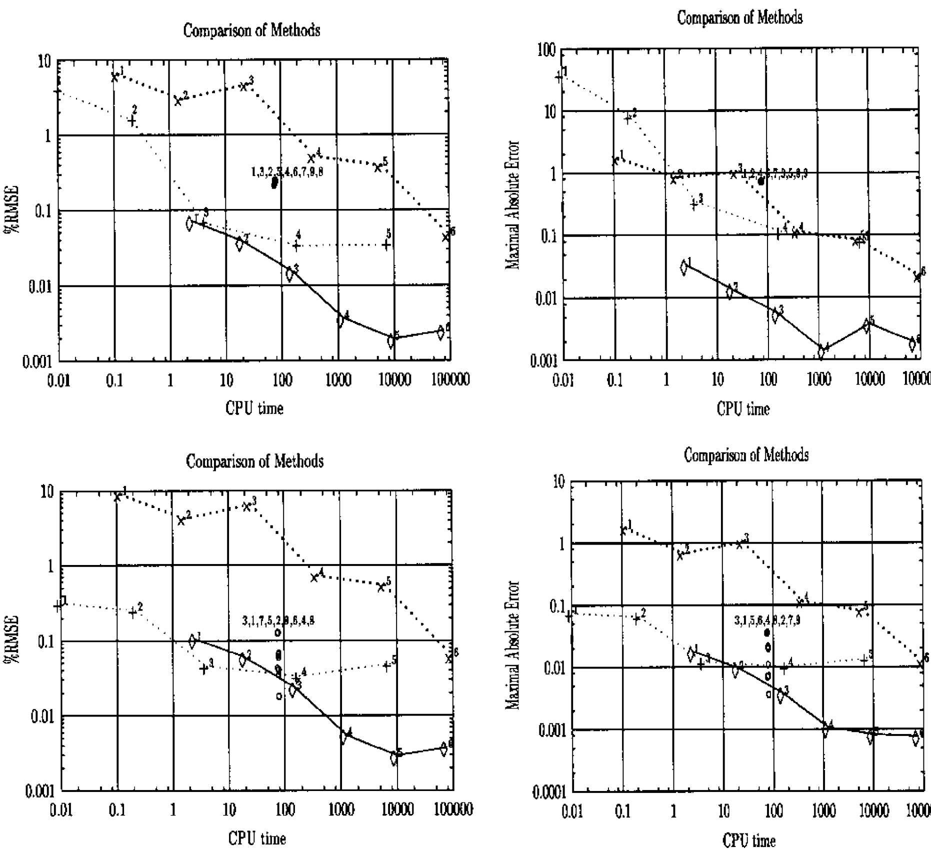

Figure 8. Comparison of numerical methods. Efficiency plots: RMSE (root mean square relative errors) versus CPU time (left panels), MAE (maximal absolute errors) versus CPU time (right panels). Top: R (risk aversion) = 0.5 to 5 and T (horizon) = 1 to 10. Bottom: $R = 5.5$ and $T = 1$ to 10. $\diamondsuit^i$: Malliavin derivatives (MCMD): $N = 10 \times 2^{i-1}$ and $M = 1000 \times 2^{2(i-1)}$. $\times^i$: Covariation (MCC): $N = 10 \times 2^{i-1}$, $M = 100 \times 2^{3(i-1)}$ and $h = 0.1/2^{i-1}$. $+^i$: Explicit (PDEFD-E): $N = 10 \times 2^{i-1}$ and $M = h = [M_\theta, M_r, M_p] = 2 \times 2^i[1, 1, 1]$. $\bigcirc^i$: Crank–Nicholson (PDEFD-CN): $N = 2+i$ and $M = h = [M_\theta, M_r, M_p] = (2+i)[1, 1, 1]$.

The comparison of MCMD and PDEFD-E shows that MCMD is more efficient if the time discretization is sufficiently large $N \geq 10$. PDEFD-E initially performs poorly, since we are close to the region where it is unstable. Unfortunately, the PDEFD-CN method is by design such that the convergence does not show in the graph. Because of its memory requirement (see discussion above), the CPU time explodes if we choose space discretizations with min $\{M_\theta, M_r, M_p\} \geq 12$, since we have to rebuild the system matrix at each time step.

VIII. Conclusions

In this paper, we have developed a comprehensive approach for the calculation of optimal portfolios in asset allocation problems with complete markets. The major benefit of our method, which relies on Monte Carlo simulation, is its flexibility. Indeed, the approach permits (i) any finite number of state variables, (ii) any diffusion process for the state variables, and (iii) any number of risky assets. It is also valid for any preference relation in the von Neumann–Morgenstern class. This flexibility provides a distinct advantage over alternative approaches to the problem.

The paper has also derived a number of economic results that can be used as guidelines for sound asset allocation rules. Naturally, the performance of these rules will also depend on the empirical sophistication of the underlying model of financial markets. Clearly, we do not suggest that the models investigated here are adequate in that respect, although they appear more realistic that the specifications examined in the prior literature. But the important point here is that the approach that we have proposed offers great generality: It can be easily adapted to address the asset allocation problem for a large class of financial market models.

Appendix A: Proofs

PROOF OF THEOREM 1: Since the Ocone and Karatzas (1991) formula is the foundation of the numerical approach in this paper, we sketch its derivation in the course of this proof.

It follows, from Cox and Huang (1989) and Karatzas et al. (1987), that optimal terminal wealth is given by $X_T = I(y\xi_T)^+ = \max(I(y\xi_T), 0)$, where $I = [u']^{-1}$ is the inverse marginal utility and y satisfies the static budget constraint $\mathbf{E}[\xi_T I(y\xi_T)^+] = x$.

Thus, optimal wealth at time t is $\xi_t X_t = \mathbf{E}_t[\xi_T X_T] = \mathbf{E}[\xi_T I(y\xi_T)^+]$. By Ito's lemma, the volatility of the left-hand side of this equation is $-\xi_t X_t \theta_t' + \xi_t X_t \pi_t' \sigma_t$. An application of the Clark–Ocone formula (see Appendix D) shows that the volatility of the right-hand side equals $\mathbf{E}_t\left[\mathcal{D}_t\left(\xi_T I(y\xi_T)^+\right)\right]$. Equating these two expressions and solving for the optimal portfolio yields

$$\xi_t X_t \pi_t' = \xi_t X_t \theta_t' \sigma_t^{-1} + \mathbf{E}_t\left[\mathcal{D}_t\left(\xi_T I(y\xi_T)^+\right)\right]\sigma_t^{-1}.$$

The chain rule of Malliavin calculus for Lipschitz functions (Nualart (1995, pp. 30–31)) gives

$$\mathcal{D}_t\big(\xi_T I(y\xi_T)^+\big) = \big(I(y\xi_T)^+ + y\xi_T I'(y\xi_T)1_{I(y\xi_T)>0}\big)\mathcal{D}_t\xi_T \equiv Z(y\xi_T)\mathcal{D}_t\xi_T,$$

where the random variable $1_{I(y\xi_T)>0}$ is the indicator of the set $I(y\xi_T)>0$ and

$$\mathcal{D}_t\xi_T = -\xi_T\left(\theta_t' + \int_t^T \mathcal{D}_t r_s\, ds + \int_t^T (dW_s + \theta_s\, ds)'\mathcal{D}_t\theta_s\right) \equiv -\xi_T\big(\theta_t' + H_{t,T}\big).$$

Combining all these elements leads to the Ocone and Karatzas (1991) portfolio formula:

$$\begin{aligned}\xi_t X_t \pi_t' =& [\xi_t X_t - \mathbf{E}_t[\xi_T Z(y\xi_T)]]\theta(t, Y_t)'\sigma(t, Y_t)^{-1} - \mathbf{E}_t\big[\xi_T Z(y\xi_T)H_{t,T}\big]\sigma(t, Y_t)^{-1}\\ =& -\mathbf{E}_t\big[\xi_T(y\xi_T)I'(y\xi_T)1_{I(y\xi_T)>0}\big]\theta(t, Y_t)'\sigma(t, Y_t)^{-1}\\ & - \mathbf{E}_t\big[\xi_T Z(y\xi_T)H_{t,T}\big]\sigma(t, Y_t)^{-1},\end{aligned}$$

where we used $\xi_t X_t = \mathbf{E}_t[\xi_T I(y\xi_T)^+]$ and the definition of $Z(y\xi_T)$ to simplify the first bracket.

When $I(y)>0$, we have $-I'(y) = 1/[-u''(I(y))]$ (from the definition $u'(I(y)) = y$). On the event $I(y\xi_T)>0$, the first-order condition for consumption optimization states that $y\xi_T = u'(I(y\xi_T))$. It follows thatx.gif" type="gif"/›

$$-\mathbf{E}_t\big[\xi_T(y\xi_T)I'(y\xi_T)1_{I(y\xi_T)>0}\big] = \mathbf{E}_t\left[\frac{\xi_T}{R(X_T)}X_T 1_{X_T>0}\right],$$

where $R(x) \equiv -u''(x)x/u'(x)$ is the relative risk aversion of the investor. Similarly, we can write

$$Z(y\xi_T) = I(y\xi_T)^+ + y\xi_T I'(y\xi_T)1_{I(y\xi_T)>0} = X_T\left[1 - R(X_T)^{-1}\right]1_{X_T>0}.$$

Substituting these expressions in the portfolio formula and rearranging gives

$$\begin{aligned}\pi_t' =& \frac{1}{R(X_t)}\mathbf{E}_t\left[\xi_{t,T}\frac{X_T}{X_t}\frac{R(X_t)}{R(X_T)}1_{X_T}>0\right]\theta_t'\sigma_t^{-1}\\ & - \mathbf{E}_t\left[\xi_{t,T}\frac{X_T}{X_t}\left(1 - R(X_T)^{-1}\right)1_{X_T}>0\int_t^T \mathcal{D}_t r_s\, ds\right]\sigma_t^{-1}\\ & - \mathbf{E}_t\left[\xi_{t,T}\frac{X_T}{X_t}\left(1 - R(X_T)^{-1}\right)1_{X_T}>0\int_t^T (dW_s + \theta_s\, ds)'\mathcal{D}_t\theta_s\right]\sigma_t^{-1}.\end{aligned}$$

Now note that the chain rule of Malliavin calculus gives

$$\begin{cases}\mathcal{D}_t\theta_s = \partial_2\theta(s, Y_s)\mathcal{D}_t Y_s\\ \mathcal{D}_t r_s = \partial_2 r(s, Y_s)\mathcal{D}_t Y_s\end{cases}. \tag{A1}$$

Furthermore (1) and Nualart (1995), Section 2.2, pp. 99–108 (see also Appendix D), imply that $\mathcal{D}_t Y_s = (\mathcal{D}_{1t}Y_s, \ldots, \mathcal{D}_{dt}Y_s)$ solves the d systems (one for each of the d

Malliavin derivatives) of d stochastic integral equations

$$\begin{aligned}\mathcal{D}_{kt}Y_s =& \mathcal{D}_{kt}Y_t + \int_t^s \mathcal{D}_{kt}\mu^Y(v,\ Y_v)dv + \int_t^s \mathcal{D}_{kt}\left(\sum_{j=1}^d \sigma^Y_{\cdot j}(v,\ Y_v)dW_{jv}\right)\\ =& \sigma^Y_{\cdot k}(t,\ Y_t) + \int_t^s \partial_2\mu^Y(v,\ Y_v)\mathcal{D}_{kt}Y_v\,dv + \int_t^s\left(\sum_{j=1}^d \partial_2\sigma^Y_{\cdot j}(v,\ Y_v)\mathcal{D}_{kt}Y_v\,dW_{jv}\right)\\ =& \sigma^Y_{\cdot k}(t,\ Y_t) + \int_t^s \partial_2\mu^Y(v,\ Y_v)\mathcal{D}_{kt}Y_v\,dv + \int_t^s\left(\sum_{j=1}^d \partial_2\sigma^Y_{\cdot j}(v,\ Y_v)dW_{jv}\right)\mathcal{D}_{kt}Y_v\end{aligned}$$

for $k = 1, \ldots, d$. Writing these equations in differential form gives (11). The initial condition $\lim_{s\to t}\mathcal{D}_{kt}Y_s = \sigma^Y_{\cdot k}(t,\ Y_t)$ follows from the integral equation above.

Remark a-1: The solution of the system of linear equations (11) could also be written in the form $\mathcal{D}_tY_s = \sigma^Y(t,\ Y_t)\exp\left\{\int_t^s dL_v\right\}$, where the $d\times d$ random variable dL_v is given by

$$dL_v \equiv \left[\partial_2\mu^Y(v,\ Y_v) - \frac{1}{2}\sum_{j=1}^d \partial_2\sigma^Y_{\cdot j}(v,\ Y_v)(\partial_2\sigma^Y_{\cdot j}(v,\ Y_v))'\right]dv + \sum_{j=1}^d \partial_2\sigma^Y_{\cdot j}(v,\ Y_v)dW_{jv}$$

and $\exp\left\{\int_t^s dL_v\right\}$ is interpreted as the exponential of a matrix (i.e., the expression for $\mathcal{D}_tY_s$ is shorthand notation for the solution of $d\mathcal{D}_tY_s = \left(dL_s + \frac{1}{2}d[L]_s\right)\mathcal{D}_tY_s$ subject to the boundary condition $\mathcal{D}_tY_t = \sigma^Y(t,\ Y_t)$, where $[L]$ is the quadratic variation process).

Proof of proposition 2: Following Doss (1977), we consider a function $F:[0,\ T]\times\mathbb{R}\mapsto\mathbb{R}$, such that $\partial_2F = \frac{1}{\sigma}$. Define the new state variable $Z_t\equiv F(t,\ Y_t)$. Using $\partial_{22}F = \partial_2(1/\sigma) = -\partial_2\sigma/\sigma^2$ and Ito's lemma implies

$$dZ_t = \left[\frac{\mu}{\sigma} - \frac{1}{2}\partial_2\sigma + \partial_1F\right](t,\ Y_t)dt + dW_t, \quad Z_0 = F(0,\ Y_0). \tag{A2}$$

Since F has an inverse, denoted by G, we can write $Y_t = G(t,\ Z_t)$. Substituting in (A2) gives $dZ_t = m(t,\ Z_t)dt + dW_t$ where $m(t,\ Z_+) \equiv \left[\mu/\sigma - \frac{1}{2}\partial_2\sigma + \partial_1F\right](t,\ G(t,\ Z_t))$ is the drift of (A2) evaluated at $Y_t = G(t, Z_t)$. Assumptions (i) and (ii) ensure that G and m is continuously differentiable. Assumption (iii) ensures that Theorem 2.2.1 of Nualart (1995) can be applied to conclude that the process Z is in the domain of the Malliavin derivative operator, that is, $Z\in\mathbb{D}^{1,2}$. Taking the Malliavin derivative on both sides of (A2) and using $\mathcal{D}_tY_s = \partial_2G(s,\ Z_s)\mathcal{D}_tZ_s$ gives

$$d\mathcal{D}_tZ_s = \partial_2m(s,\ Z_s)\mathcal{D}_tZ_sds = \partial_2\left[\frac{\mu}{\sigma} - \frac{1}{2}\partial_2\sigma + \partial_1F\right](s,\ G(s,\ Z_s))\partial_2G(s,\ Z_s)\mathcal{D}_tZ_sds,$$

subject to the boundary condition $\mathcal{D}_tZ_t = 1$. Solving this linear SDE for $\mathcal{D}_tZ_s$ and using the relations for derivatives of F and its inverse G produces the result stated. ■

EXPRESSIONS FOR (21) IN THE BENCHMARK MODEL: Consider the case of $\delta_r = 0$. Differentiation gives,

$$\partial_2\mu_\theta(x) = -\kappa_\theta$$

$$\partial_1\sigma_\theta(x) = 0 \quad \text{and} \quad \partial_2\sigma_\theta(x) = -\frac{1}{2}\varepsilon(x)\frac{\sigma_\theta(x)}{x}$$

$$\partial_{22}\sigma_\theta(x) = \frac{1}{2}\varepsilon(x)\frac{\sigma_\theta(x)}{x}\left(\frac{\varepsilon(x)}{2x} + \frac{1}{\theta_l + x}\right) - \frac{\gamma_{20}(1-\gamma_{10})^2}{\theta_l + \theta_u}\frac{\sigma_\theta(x)}{\theta_l + x}\frac{\left(\frac{\theta_l + x}{\theta_l + \theta_u}\right)^{-\gamma_{2\theta}}}{\left(1 - \left(\frac{\theta_l + x}{\theta_l + \theta_u}\right)^{1-\gamma_{2\theta}}\right)^2}$$

(corresponding expressions can be derived for $\mathcal{D}_t r_s$). ■

Appendix B: Asymptotic Laws of State Variables Estimators

This appendix reports results from DGR (2001) on the asymptotic laws of estimators of the state variables. Let Z_t be the vector of state variables after the Doss transformation. It satisfies $dZ_t = m(Z_t)dt + \sum_{j=1}^{d} dW_t^j$ (see equation (A2) in the univariate case). Using the Euler scheme gives an estimator Z_T^N of Z_T. Our next theorem characterizes the estimation error.

THEOREM B-1: *The asymptotic law of the estimator of the state variables Z is given by* $U_{t,T}^{Z^N} \equiv N(Z_T^N - Z_T) \Rightarrow U_{t,T}^Z$, *where*

$$U_{t,T}^Z = -\hat{\Omega}_{t,T}\int_t^T \hat{\Omega}_{t,s}^{-1}\partial m(Z_t) \times\left[\frac{1}{2}\left(m(Z_t)dt + \sum_{j=1}^{d} dW_t^j\right) + \frac{1}{\sqrt{12}}\sum_{j=1}^{d} dB_v^j + \frac{1}{2}\sum_{k,l=1}^{d}\partial_{lk}m(Z_s)ds\right]$$

with $\hat{\Omega}_{t,v} = \exp\left(\int_t^v \partial m(Z_s)ds\right)$ *and with* $[B^j]_{j\in\{1,\ldots,d\}}$ *a* $d\times 1$ *standard Brownian motion independent of W.*

Theorem B-1 provides an explicit expression for the asymptotic law of the estimator and shows that the speed of convergence is of order $1/N$. These results can be contrasted with those obtained when state variables are estimated before transformation. Applying a Euler scheme to estimate the solution of (1) gives $U_t^{Y^N} \equiv \sqrt{N}(Y_t^N - Y_t) \Rightarrow U_t^Y$, where

$$U_{t,v}^Y = -\frac{1}{\sqrt{2}}\Omega_{t,v}\int_t^v \Omega_{t,s}^{-1}\sum_{h,j=1}^{d}[(\partial\sigma_{\cdot j}^Y)\sigma_{\cdot h}^Y](Y_s)dB_s^{h,j}$$

with

$$\Omega_{t,v} = \exp\left(\int_t^v [\partial\mu^Y(Y_s) - \frac{1}{2}\sum_{j=1}^{d}(\partial\sigma_{\cdot j}^Y(Y_s))^2]ds + \sum_{j=1}^{d}\int_t^v \partial\sigma_{\cdot j}^Y(Y_s)dW_s^j\right)$$

and where the processes $[B^{h,j}]_{h,\ j\in\{1,\ldots,\ d\}}$ are standard Brownian motions independent of W.

In this case, the speed of convergence is $1/\sqrt{N}$. Theorem B1 illustrates the increase in the speed of convergence achieved by using the Doss transformation. It also shows that the limit law is different and involves an exponential of a bounded variation process instead of a stochastic integral. DGR (2001) provides additional results for conditional expectations of functionals of state variables such as those in the hedging terms $a(t, Y_t)$ and $b(t, Y_t)$. The increased rate of convergence is important when computing estimators of these conditional expectations based on an approximation of the dynamic evolution of the state variables.

Appendix C: Calibration of the Benchmark Model

We focus on a constrained version of our benchmark IR-MPR model (23) and (24) with $\gamma_{1\theta} = 0.5$, $\theta_l = \theta_u = 1.5$. To calibrate the model, we assume that the approximate discrete-time process is the true time-series model.[25] The econometric procedure described in this section is based on the maximization of the log-likelihood of the following discrete-time model

$$r_{t_{n+1}}^{(h)} = r_{t_n}^{(h)} + \kappa_r(\bar{r}_h - r_{t_n}^{(h)})(1 + \phi_{r,h}(\bar{r}_h - r_{t_m}^{(h)})^{2\eta_r}) + \sigma_{r,h}(r_{t_n}^{(h)})^{\gamma_r}\varepsilon_{t_{n+1}}, \quad r_0 \text{ given} \quad \text{(C1)}$$

$$\begin{aligned}\theta_{t_{n+1}} =& \theta_{t_n} + \kappa_\theta(\bar{\theta} - \theta_{t_n}) + \delta_{\theta,h}(\bar{r}_h - r_{t_n}^{(h)})(1.5 + \theta_{t_n})\left(1 - \left(\frac{1.5 + \theta_{t_n}}{3}\right)\right) \\ &+ \sigma_\theta(1.5 + \theta_{t_n})^{0.5}\left(1 - \left(\frac{1.5 + \theta_{t_n}}{3}\right)^{0.5}\right)^{\gamma_{2\theta}} \cdot v_{t_{n+1}}, \quad \theta_0 \text{ given,}\end{aligned} \quad \text{(C2)}$$

where $\bar{r}_h = \bar{r}h$, $\sigma_{r,h} = \sigma_r h^{(1-\gamma_r)}$, $\phi_{r,h} = \phi_r h^{-2\eta_r}$, and $\delta_{\theta,h} = \delta_\theta h$, and $\{t_n: n = 0, \ldots, N\}$ is a partition of $[0, T]$. In our estimations, we consider a monthly frequency with $h = 1/12$.

Since the MPR, $\theta_t = \sigma_t^{-1}(\mu_t - r_t)$, is unobservable, it must be filtered from the data. We assume that the stock volatility σ is constant. In other words, we estimate the MPR from the conditional mean μ_t of the stock return series (taken as the S&P500 index), assuming a simple AR(1) process for the conditional mean. The estimation period is January 1965 to June 1996. Although in the continuous-time model the same Brownian motion applies to r and θ with a perfect negative correlation, we leave the correlation coefficient between $\varepsilon_{t_{n+1}}$ and $v_{t_{n+1}}$ unconstrained in the estimation. We obtained the following results: $\kappa_r = 0.0027668$, $\bar{r} = 0.0063138 \times 12$, $\phi_r = 37.008/12^{2\times 0.45432}$, $\eta_r = 0.45432$, $\sigma_r = 0.154055 \times 12^{1-1.1741}$, and $\gamma_r = 1.1741$ for the parameters of the IR process, and

[25] Estimating the parameters of a continuous-time diffusion model based on a discrete-time approximation of the likelihood function leads to a discretization bias (Lo (1988)). However, for the monthly estimation of IR processes, Broze, Scaillet, and Zakoian (1995) use an indirect estimation to correct for the bias and find that it is small for the mean-reversion κ_r, the mean $\bar{r}$, and the variance σ_r. We, therefore, follow the simpler approach to calibrate the parameters.

$\kappa_\theta = 0.85576$, $\bar{\theta} = 0.048786$, $\sigma_\theta = 2.9417$, $\theta_l = 1.5$, $\theta_u = 1.5$, $\gamma_{1,\theta} = 0.5$, $\gamma_{2,\theta} = 2.8313$, and $\delta_\theta = 3.0708$ for those of the MPR process.

To evaluate the impact of nonlinearities, we also calibrated the model

$$r_{t_{n+1}}^{(h)} = r_{t_n}^{(h)} + \kappa_r(\bar{r}_h - r_{t_n}^{(h)}) + \sigma_{r,h}\sqrt{r_{t_n}^{(h)}}\varepsilon_{t_{n+1}}$$

$$\theta_{t_{n+1}} = \theta_{t_n} + \kappa_\theta(\bar{\theta} - \theta_{t_n}) + \delta_{\theta,h}(\bar{r}_h - r_{t_n}^{(h)}) + \sigma_\theta v_{t_{n+1}}, \quad \theta_0 \text{ given.}$$

The parameter estimates obtained are $\kappa_r = 0.005$, $\bar{r} = 0.005\times 12$, $\sigma_r = 0.03637$, $\kappa_\theta = 0.77706$, $\bar{\theta} = 0.2675$, $\sigma_\theta = 0.2005$, and $\delta_\theta = 2.1667$.

To assess the robustness of the results assuming a constant σ, we used a GARCH (1,1) model for the stock returns to construct the series for the MPR θ_t while keeping an AR(1) specification for the conditional mean of the stock returns. The estimates are not changed much and lead to comparable hedging and portfolio shares.

For the specification with dividends, the discrete-time model is (C1) for the IR and

$$\begin{aligned}\theta_{t_{n+1}} =& \theta_{t_n} + \kappa_\theta(\bar{\theta} - \theta_{t_n}) + \delta_{r,h}(\bar{r}_h - r_{t_n}^{(h)})(1.5 + \theta_{t_n})\left(1 - \left(\frac{1.5 + \theta_{t_n}}{3}\right)\right) \\ &+ \delta_{p,h} - \bar{p}_h - p_{t_n}^{(h)})(1.5 + \theta_{t_n})\left(1 - \left(\frac{1.5 + \theta_{t_n}}{3}\right)\right) \\ &+ \sigma_\theta(1.5 + \theta_{t_n})^{0.5}\left(1 - \left(\frac{1.5 + \theta_{t_n}}{3}\right)^{0.5}\right)^{\gamma_{2\theta}} \cdot v_{t_{n+1}}, \quad \theta_0 \text{given,}\end{aligned}$$

$$p_{t_n+1}^{(h)} = p_{t_n}^{(h)} + \kappa_p(\bar{p}_h - p_{t_n}^{(h)})(1 + \phi_{p,h}(\bar{p}_h - p_t^{(h)})^{2\eta_p}) + \sigma_{p,h}(p_{t_n}^{(h)})^{\gamma_p}\varepsilon_{t_{n+1}}, \quad p_0 \text{ given}$$

for the MPR and DPR. Here $\delta_{r,h} = \delta_r h$, $\bar{p}_h = \bar{p}h$, $\sigma_{p,h} = \sigma_p h^{(1-\gamma_r)}$, $\phi_{p,h} = \phi_p h^{-2v_r}$, $\delta_{p,h} = \delta_p h$, and $\{t_n : n = 0,\ldots,N\}$ is a partition of $[0, T]$. The estimated parameter values are $\kappa_r = 0.007185$, $\bar{r} = 0.00407\times 12$, $\phi_r = 54.45/12^{2\times 0.3601}$, $\eta_r = 0.3601$, $\gamma_r = 0.716$, $\sigma_r = 0.0146\times 12^{1-0.716}$, $\kappa_\theta = 0.989$, $\bar{\theta} = 0.119$, $\theta_l = 1.5$, $\theta_u = 1.5$, $\gamma_{1,\theta} = 0.5$, $\gamma_{2,\theta} = 0.659$, $\delta_{r\theta} = 32.47/12$, $\delta_{p\theta} = -17.46/12$, $\sigma_\theta = 0.1626$, $\kappa_p = 0.020$, $\bar{p} = 0.0032\times 12$, $\phi_p = 20.93/12^{2\times 0.244}$, $\eta_p = 0.244$, $\gamma_p = 0.6315$, and $\sigma_p = 0.005\times 12^{1-0.6315}$.

We proceed similarly for the model with four asset classes from 1971 to 1999. The parameter values are the following.

For the IR: $\kappa_r = 0.00034$, $\bar{r} = 0.00520\times 12$, $\phi_r = 17224.987/12^{2\times 0.4116}$, $\eta_r = 0.4116$, $\gamma_r = 0.5664$, $\sigma_r = 0.00986\times 12^{1-0.5664}$.

For the MPRs: $\kappa_1 = 0.1219$, $\kappa_2 = 0.5946$, $\kappa_3 = 0.7483$, $\bar{\theta}_1 = 0.1562$, $\bar{\theta}_2 = 0.4251$, $\bar{\theta}_3 = 0.1669$, $\theta_{l1} = \theta_{l2} = \theta_{u1} = \theta_{u2} = 1.5$, $\theta_{l3} = \theta_{u3} = 2.5$, $\delta_{1r} = -2.7648/12$, $\delta_{2r} = 139.00/12$, $\delta_{3r} = 176.76/12$, $\delta_{1p} = -0.0372$, $\delta_{2p} = 14.04$, $\delta_{3p} = -4.44$, $\sigma_{11} = -0.2032$, $\sigma_{12} = 0.00497$, $\sigma_{13} = 0.0356$, $\sigma_{21} = -0.1237$, $\sigma_{22} = -0.0306$, $\sigma_{23} = 0.0406$, $\sigma_{31} = -0.1199$, $\sigma_{32} = -0.493$, $\sigma_{33} = 0.402$, $\gamma_{1,\theta_1} = \gamma_{1,\theta_2} = \gamma_{1,\theta_3} = 0.5$, $\gamma_{2,\theta_1} = 1.2158$, $\gamma_{2,\theta_2} = 0.5095$, $\gamma_{2,\theta_3} = 0.6440$.

For the DPR: $\kappa_p = 0.005$, $\bar{p} = 0.0332\times 12$, $\phi_p = 0$, $\eta_p = 0$, $\sigma_{p1} = -0.00103\times 12^{1-0.5}$, $\sigma_{p2} = 0.01011\times 12^{1-0.5}$, $\sigma_{p3} = 0.003\times 12^{1-0.5}$, $\gamma_p = 0.5$.

For the volatility of prices and their correlations, we obtained: $\sigma_0 = 0.156$, $\rho_0 = 0.37$, $\sigma_n = 0.229$, $\rho_{n1} = 0.32$, $\rho_{n2} = -0.1274$, $\sigma_1 = 0.106$.

Appendix D: Elements of Malliavin Calculus for Finance

The Malliavin calculus is a calculus of variations for stochastic processes defined on a Wiener space. It applies to random variables and stochastic processes that depend on the trajectories of a Brownian motion, that is, Wiener functionals. In many contexts, one needs to measure the effects of a small variation in the trajectory of the underlying Brownian motion on this functional. Malliavin calculus gives the necessary tools to perform this computation.

Let $(t_1, \ldots, t_n)$ be a partition of $[0, T]$ and let F be a random variable of the form

$$F \equiv f(W_{t_1}, \ldots, W_{t_n}),$$

where f is a continuously differentiable function. The random variable F depends on the Brownian motion W at a finite number of points along its sample path; it is called a *smooth Brownian functional.*

The Malliavin derivative of F is the change in F due to a change in the path of W. Specifically, consider a time t such that $t_1 < \ldots < t_{k-1} < t \leq t_k \ldots < t_n$ and suppose that we perturbate W_s to $W_s + \varepsilon$ for all $s \geq t$. The Malliavin derivative of F at t, denoted by $\mathcal{D}_t F$, is defined as

$$\begin{aligned} \mathcal{D}_t F &\equiv \left. \frac{\partial f(W_{t_1}, \ldots, W_{t_{k-1}}, W_{t_k} + \varepsilon, \ldots, W_{t_n} + \varepsilon)}{\partial \varepsilon} \right|_{\varepsilon=0} \\ &= \sum_{i=k}^{n} f_i(W_{t_1}, \ldots, W_{t_k}, \ldots, W_{t_n}), \end{aligned}$$

where f_i is the derivative with respect to the i^{th} argument of f.

A simple example is that of a lognormal price process $S_T = S_0 \exp(\alpha T + \sigma W_T)$, where α, σ are constants. A direct application of the definition gives

$$\mathcal{D}_t S_T = \frac{\partial S_T}{\partial W_T} = \sigma S_0 \exp(\alpha T + \sigma W_T) = \sigma S_T.$$

In this case, S_T depends only on the Brownian motion at time T. The Malliavin derivative is then the derivative with respect to W_T. This reflects the fact that a perturbation of the path of the Brownian motion from t onward affects S_T only through the terminal value W_T.

The definition above can be extended to random variables that depend on the path of the Brownian motion over a continuous interval $[0, T]$. This extension uses the fact that a path-dependent functional can be approximated by a suitable sequence of smooth Brownian functionals. In essence, the Malliavin derivative of the path-dependent functional is the limit of the Malliavin derivatives of the smooth Brownian functionals in the approximating sequence.

The space of random variables for which Malliavin derivatives are defined is called $\mathbb{D}^{1,2}$.[26]

This extension enables us to define Malliavin derivatives of stochastic integrals in a natural manner. For instance, consider the stochastic integral $F = \int_0^T h(t)dW_t$, where $h(t)$ is a function of time. We have $\mathcal{D}_t F = h(t)$, that is, the Malliavin derivative of F at date t is the volatility $h(t)$ of the stochastic integral at t. It measures the sensitivity of the random variable F to the Brownian innovation at t.

For practical purposes, we need to be able to compute the Malliavin derivative of a function of a path-dependent random variable. As in ordinary calculus, a chain rule also applies in Malliavin calculus. Let $F = (F_1, \ldots, F_n)$ be a vector of random variables in $\mathbb{D}^{1,2}$, and suppose that ϕ is a differentiable function of F with bounded derivatives. Then,

$$\mathcal{D}_t\phi(F) = \sum_{i=1}^{n} \frac{\partial\phi}{\partial x_i}(F)\mathcal{D}_t F_i.$$

In particular for the Riemann integral with path-dependent integrand $F = \int_0^T x(s)ds$ where $x(\cdot)$ is a progressively measurable bounded process, we obtain $\mathcal{D}_t F = \int_t^T \mathcal{D}_t x(s)ds$. Similarly, for the stochastic integral with path-dependent integrand $F = \int_0^T x(s)dW_s$, we have $\mathcal{D}_t F = \int_t^T \mathcal{D}_t x(s)dW_s + x(t)$.

These formulas help us to identify the Malliavin derivative of a process that satisfies a stochastic differential equation, as in our portfolio problem. Suppose that a state variable Y_t follows the diffusion process $dY_t = \mu(Y_t)dt + \sigma(Y_t)dW_t$, where Y_0 is given. Equivalently, we can write the process Y_t in integral form as

$$Y_t = Y_0 + \int_0^t \mu(Y_s)ds + \int_0^t \sigma(Y_s)dW_s.$$

Using the results above, it is easy to see that the Malliavin derivative $\mathcal{D}_t Y_s$ satisfies

$$\mathcal{D}_t Y_s = \mathcal{D}_t Y_0 + \int_t^s \frac{\partial\mu}{\partial Y}\mathcal{D}_t Y_v dv + \int_t^s \frac{\partial\sigma}{\partial Y}\mathcal{D}_t Y_v dW_v + \sigma(Y_t).$$

Since $\mathcal{D}_t Y_0 = 0$, the Malliavin derivative obeys the following linear SDE

$$d(\mathcal{D}_t Y_s) = \frac{\partial\mu(Y_s)}{\partial Y}(\mathcal{D}_t Y_s)ds + \frac{\partial\sigma(Y_s)}{\partial Y}(\mathcal{D}_t Y_s)dW_s$$

subject to the initial condition $\lim_{s\to t}\mathcal{D}_t Y_s = \sigma(Y_t)$. As for any stochastic differential equation, the solution (i.e., the Malliavin derivative) can be simulated by Monte Carlo methods.

It is well known that martingales, in Brownian spaces, can be written as sums of Brownian motions. This result is the martingale representation theorem. One

[26] The Malliavin derivative is defined on the space $\mathbb{D}^{1,2}$ which is the completion of the set of smooth Brownian functionals with respect to the norm $\| F \|_{1,2} = \left(E(F^2)\right)^{1/2} + \left(E\left(\int_0^T \|\mathcal{D}_t F\|^2 dt\right)\right)^{1/2}$.

benefit of Malliavin calculus is that it gives an explicit expression for the integrand that appears in this representation formula, that is, it identifies the volatility coefficient of the martingale. This is the Clark–Ocone formula, which states that any random variable $F \in \mathbb{D}^{1,2}$ can be decomposed as

$$F = E(F) + \int_0^T E[\mathcal{D}_t F|\mathcal{F}_t]dW_t,$$

where $\mathcal{F}_t$ represents the information generated by the Brownian motion W up to t.

Ocone and Karatzas (1991) extended this formula to processes that are martingales under an equivalent measure (such as the risk-neutral measure) and used the result to derive their portfolio formula. A full treatment of Malliavin calculus can be found in Nualart (1995).

REFERENCES

Ahn, Dong-Hyun, and Bin Gao, 1999, A parametric nonlinear model of term structure dynamics, *Review of Financial Studies* 12, 721–762.

Ait-Sahalia, Yacine, 1996, Testing continuous-time models of the spot interest rate, *Review of Financial Studies* 9, 385–426.

Ait-Sahalia, Yacine, and Michael W. Brandt, 2001, Variable selection for portfolio choice, *Journal of Finance* 56, 1297–1351.

Arrow, Kenneth J., 1975, *Essays in the Theory of Risk-Bearing* (Markham Press, Chicago).

Balduzzi, Pierluigi, and Anthony W. Lynch, 1999, Transaction costs and predictability: Some utility cost calculations, *Journal of Financial Economics* 52, 47–78.

Barberis, Nicholas, 2000, Investing for the long run when returns are predictable, *Journal of Finance* 55, 225–264.

Brandt, Michael W., 1999, Estimating portfolio and consumption choice: A conditional Euler equations approach, *Journal of Finance* 54, 1609–1645.

Brandt, Michael W., Amit Goyal, and Pedro Santa-Clara, 2001, A simulation approach to dynamic portfolio choice with an application to industry momentum, Working paper, Wharton School.

Brennan, Michael J., 1998, The role of learning in dynamic portfolio decisions, *European Finance Review* 1, 295–306.

Brennan, Michael, Eduardo Schwartz, and Ronald Lagnado, 1997, Strategic asset allocation, *Journal of Economic Dynamics and Control* 21, 1377–1403.

Brennan, Michael J., and Yihong Xia, 2001, Dynamic asset allocation under inflation, *Journal of Finance* 57, 1201–1238.

Broze, Laurence, Olivier Scaillet, and Jean-Michel Zakoian, 1995, Testing for continuous-time models of the short-term interest rate, *Journal of Empirical Finance* 2, 199–223.

Campbell, John Y., Jorge Rodriguez, and Luis M. Viceira, 2001, Strategic asset allocation in a continuous-time VAR model, Working paper, Harvard University.

Campbell, John Y., and Luis M. Viceira, 1999, Consumption and portfolio decisions when expected returns are time varying, *Quarterly Journal of Economics* 114, 433–495.

Campbell, John Y., and Luis M. Viceira, 2001, Who should buy long-term bonds? *American Economic Review* 91, 99–127.

Chacko, George, and Luis M. Viceira, 1999, Dynamic consumption and portfolio choice with stochastic volatility in incomplete markets, Working paper, Harvard University.

Chan, Kalok C., Andrew Karolyi, Francis Longstaff, and Anthony B. Sanders, 1992, An empirical comparison of alternative models of the short-term interest rate, *Journal of Finance* 47, 1209–1227.

Clément, Emmanuelle, Damien Lamberton, and Philip Protter, 2002, An analysis of the Longstaff-Schwartz algorithm for American option pricing, *Finance and Stochastics* 6, 449–471.

Cox, John C., and Chi-fu Huang, 1989, Optimal consumption and portfolio policies when asset prices follow a diffusion process, *Journal of Economic Theory* 49, 33–83.

Cox, John C., Jonathan E. Ingersoll, and Steve A. Ross, 1985, An intertemporal general equilibrium model of asset prices, *Econometrica* 53, 363–384.

Cox, John C., and Steve A. Ross, 1976, The valuation of options for alternative stochastic processes, *Journal of Financial Economics* 3, 145–166.

Cvitanic, Jaksa, Levon Goukasian, and Fernando Zapatero, 2003, Monte Carlo computation of optimal portfolios in complete markets, *Journal of Economic Dynamics and Control* 27, 971–986.

Dammon, Robert M., Chester S. Spatt, and Harold H. Zhang, 2001, Optimal consumption and investment with capital gains taxes, *Review of Financial Studies* 14, 583–616.

Detemple, Jérôme B., René Garcia, and Marcel Rindisbacher, 2001, Asymptotic properties of Monte Carlo estimators of diffusion processes, Working paper, CIRANO.

Doss, Halim, 1977, Liens entre équations différentielles stochastiques et ordinaires, *Annales de l'Institut Henri Poincaré* 13, 99–125.

Heston, Steve, and Guofu Zhou, 2001, On the rate of convergence of discrete-time contingent claims, *Mathematical Finance* 10, 53–75.

Karatzas, Ioannis, John P. Lehoczky, and Steve E. Shreve, 1987, Optimal portfolio and consumption decisions for a "small investor" on a finite horizon, *SIAM Journal of Control and Optimization* 25, 1557–1586.

Kim, Tong Suk, and Edward Omberg, 1996, Dynamic nonmyopic portfolio behavior, *Review of Financial Studies* 9, 141–161.

Kogan, Leonid, and Raman Uppal, 2000, Risk aversion and optimal portfolio policies in partial and general equilibrium economies, Working paper, University of Pennsylvania.

Kurtz, Thomas G., and Philip Protter, 1991, Wong-Zakai corrections, random evolutions and numerical schemes for SDE's, in *Stochastic Analysis* Liber amicorum for Moshe Zakai, edited by Eddy Mayer-Wolf, Ely Merzbach, and Adam Shwartz, Academic Press, Boston 331–346.

Lioui, Abraham, and Patrick Poncet, 2001, On optimal portfolio choice under stochastic interest rates, *Journal of Economic Dynamics and Control* 25, 1841–1865.

Liu, Jun, 2001, Portfolio selection in stochastic environments, Working paper, UCLA.

Lo, Andrew W., 1988, Maximum likelihood estimation of generalized Ito processes with discretely-sampled data, *Econometric Theory* 4, 231–247.

Longstaff, Francis, and Eduardo Schwartz, 2001, Valuing American options by simulation: A simple least-squares approach, *Review of Financial Studies* 14, 113–147.

Markowitz, Harry, 1952, Portfolio selection, *Journal of Finance* 7, 77–91.

Merton, Robert C., 1969, Lifetime portfolio selection under uncertainty: The continuous-time case, *Review of Economics and Statistics* 51, 247–257.

Merton, Robert C., 1971, Optimum consumption and portfolio rules in a continuous time model, *Journal of Economic Theory* 3, 273–413.

Nualart, David, 1995. *The Malliavin Calculus and Related Topics* (Springer Verlag, New York).

Ocone, Daniel, and Ioannis Karatzas, 1991, A generalized Clark representation formula, with application to optimal portfolios, *Stochastics and Stochastics Reports* 34, 187–220.

Pliska, Stanley, 1986, A stochastic calculus model of continuous trading: Optimal portfolios, *Mathematics of Operations Research* 11, 371–382.

Richard, Scott F., 1975, Optimal consumption, portfolio, and life insurance rules for an uncertain lived individual in a continuous-time model, *Journal of Financial Economics* 2, 187–203.

Samuelson, Paul A., 1969, Lifetime portfolio selection by dynamic stochastic programming, *Review of Economics and Statistics* 51, 239–246.

Schroder, Mark, and Costis Skiadas, 1999, Optimal consumption and portfolio selection with stochastic differential utility, *Journal of Economic Theory* 89, 68–126.

Wachter, Jessica, 2002, Optimal consumption and portfolio allocation under mean-reverting returns: An exact solution for complete markets. *Journal of Financial and Quantitative Analysis* 37, 63–91.